



Research article

Effects of phthalic acid esters released from long-term agricultural film mulching on soil properties, bacterial communities, and functions in Xinjiang cotton field



Yuanyang Yi ^a, Yuxian Wang ^b, Jing Zhu ^c, Meiyi Gu ^c, Jianwei Chen ^d , Ling Jiang ^e, Delong Kong ^a, Zhidong Zhang ^{a,c,*}, Wei Zhang ^{a,**}

^a School of Life Sciences, Xinjiang Normal University, Urumqi, 830046, China

^b Xinjiang Key Laboratory of Biological Resources and Genetic Engineering, College of Life Science and Technology, Xinjiang University, Urumqi, 830017, China

^c Xinjiang Key Laboratory of Special Environmental Microbiology, Institute of Microbiology, Xinjiang Academy of Agricultural Sciences, Urumqi, 830091, China

^d BGI Research, Qingdao, 266426, China

^e State Key Laboratory of Materials-Oriented Chemical Engineering, College of Food Science and Light Industry, Nanjing Tech University, Nanjing, 211816, China

ARTICLE INFO

Keywords:

Phthalic acid esters
Agricultural film mulching
Soil enzymes
Bacterial community
Long-term ecological effects

ABSTRACT

The global use of transparent agricultural films has raised significant concerns about the contamination of phthalate esters (PAEs). Despite these concerns, field studies on PAE accumulation due to long-term agricultural film use remain limited. This study focuses on cotton fields in Xinjiang with varying mulching durations (0–30 years) to explore the accumulation of PAEs and their effects on soil physicochemical properties, enzyme activities, microbial metabolic functions, and community structure. Results reveal that with the increase in mulching duration, the Σ PAEs content in the soil did not follow a linear growth trend, but instead exhibited a pattern of initial increase followed by a decrease. The peak concentration was observed in the 8th year, reaching 6.40 mg/kg. This decline is attributed to multiple factors, including microbial adaptation, decreased film degradation, and soil uptake of residual compounds. The accumulation and degradation of PAEs significantly altered soil pH and organic matter content. Both soil enzyme activity and microbial metabolic activity showed a three-phase fluctuation over time, initially increasing, then decreasing, and finally increasing again, highlighting the microbial response to environmental PAE-induced stress. Similarly, the diversity and composition of bacterial communities exhibited analogous fluctuations. The analysis of keystone species abundance, assessment of co-occurrence network complexity, and evaluation of their ecological functions in carbon, nitrogen, and sulfur cycling collectively underscore the potential risks posed by PAEs in long-term mulched cotton fields to soil health and ecosystem stability. In summary, this study provides comprehensive field-based evidence that long-term use of agricultural mulching films leads to dynamic changes in PAEs accumulation, which in turn affect soil physicochemical properties, microbial functions, and ecosystem stability, thereby underscoring the ecological risks associated with prolonged plastic film application in agroecosystems.

1. Introduction

Phthalate esters (PAEs) are commonly used plasticizers found in a variety of applications, including food packaging, agricultural films, medical products, and cosmetics (Benjamin et al., 2015; Yang et al., 2025). Due to their non-covalent bonding with plastics and high mobility, PAEs can be easily released during production and usage

(Paluselli and Kim, 2020). Consequently, these compounds have been widely detected in diverse environments, such as the atmosphere, water bodies, and soil (Hu et al., 2021; Long et al., 2024; Sokolowski et al., 2024). Numerous studies have demonstrated that PAEs exhibit significant bioaccumulation and magnification effects (Kumari and Kaur, 2020; Li et al., 2020c), allowing them to be absorbed by plants and enter the human body through the food chain, potentially leading to toxicity

* Corresponding author. Xinjiang Key Laboratory of Special Environmental Microbiology, Institute of Microbiology, Xinjiang Academy of Agricultural Sciences, Urumqi, 830091, China.

** Corresponding author. School of Life Sciences, Xinjiang Normal University, Urumqi, 830046, China.

E-mail addresses: zhangzheedong@sohu.com (Z. Zhang), zw0991@sohu.com (W. Zhang).

in the endocrine, reproductive, and metabolic systems (Long et al., 2024). Additionally, these chemicals may exhibit mutagenic, teratogenic, and carcinogenic effects. Hence, the U.S. Environmental Protection Agency has listed six major PAE compounds as priority pollutants that should be regulated. These are dimethyl phthalate (DMP), diethyl phthalate (DEP), butyl-benzyl phthalate (BBP), di-n-butyl phthalate (DBP), di (2-ethylhexyl) phthalate (DEHP) and di-n-octyl phthalate (DnOP). (Monti et al., 2022).

Agricultural films are a significant source of PAEs contamination in farmland. While the use of agricultural films has notably increased the accumulation of organic matter in soil, promoting nutrient cycling rates and plant growth (Shi et al., 2022), the resulting PAEs pollution from long-term use of agricultural films negatively impacts soil health, potentially influencing agricultural productivity and hindering sustainable development. Therefore, studying the changes in PAE content in long-term agricultural film mulching soils and their effects on the soil ecosystem is crucial for agricultural sustainability and has garnered considerable attention from researchers. Currently, scientists such as Monti et al. (2022) and Li et al. (2016) have investigated the relationship between the duration of film mulching and changes in soil PAEs; however, these studies have generally focused on relatively short coverage periods of only a few months and have yet to explore the effects of decades of film coverage on PAEs dynamics in agricultural soils. Meanwhile, most existing studies on soil PAEs have been conducted in controlled laboratory settings, concentrating on the effect of individual PAEs. For example, Kapanen et al. (2007) examined the impacts of DEP on soil within a concentration range of $10\text{--}10^5 \text{ mg kg}^{-1}$, while Tao et al. (2021) and Huang et al. (2022) explored the effects of DBP and DEHP in the concentration range of $10\text{--}100 \text{ mg kg}^{-1}$. However, the types of PAEs present in real farmland are complex, and their concentrations typically fall below 10 mg kg^{-1} (Chen et al., 2024; Li et al., 2022a; Li et al., 2020a). The types and concentrations of pollutants used in laboratory studies differ significantly from those encountered in actual agricultural contexts, which limits our systematic understanding of the ecological impact mechanisms of PAEs under in-situ long-term accumulation conditions.

China is the largest user of agricultural mulching films in the world (Yang et al., 2023), with Xinjiang province reporting the highest usage nationally, especially in cotton cultivation (Hu et al., 2019). The residual levels of mulching films in cotton fields are 4–5 times higher than the national average, which significantly exacerbates PAE pollution (Han et al., 2025). Research has indicated that residual PAEs have significantly affected the physical functions of the soil ecosystem, such as changes in soil nutrients (e.g., available phosphorus, alkaline nitrogen, and organic matter (Zhang et al., 2023). In addition, soil microbial communities are essential for ecosystem functions, including nutrient cycling and carbon sequestration. These communities exhibit highly sensitive responses to environmental stressors, serving as critical indicators of soil health and fertility (Dincă et al., 2022). Increasing evidence suggests that the abundance, structure, and diversity of soil microbial communities are significantly impacted by the presence of PAEs, posing substantial risks to soil-crop ecosystems. For instance, Kong et al. (2018) observed that high concentrations of PAEs can cause drastic changes in the composition of local bacterial communities, affecting their abundance and structure. Kapanen et al. (2007) found that PAEs reduce microbial diversity by decreasing the richness of bacterial species and leading to a reduction of *Pseudomonas* populations by up to 62 %. Moreover, soil enzymes play a crucial role in soil metabolism and are indicators of microbial activity and soil quality. The significant impact of PAE accumulation on soil enzyme activity has also been confirmed by Gao et al. (2020), Wang et al. (2015, 2016) reported that residual plastic films in agricultural soils can inhibit soil dehydrogenase activity by up to 45 %. Currently, most research on PAEs remains focused on studying the impact of short-term film coverage on PAE concentrations (Sun et al., 2022; Uzamurera et al., 2023; Viljoen et al., 2023). Comprehensive studies on the dynamic accumulation of PAEs

over the long term and their impact on soil microbial communities have yet to be reported.

In this study, we selected actual film-mulched cotton fields with mulching durations of 0 (no film), 3, 8, 12, 15, 20, 25, and 30 years in the Caijiahu reclamation area of Wu{jiaqu}, located in the desert-oasis ecotone on the southern margin of the Junggar Basin, as the research objects. This region has scarce water resources, and is ecologically sensitive and fragile, with cotton planting areas covered with plastic film exceeding 120,000 acres year-round, and a film-covered planting history dating back 55 years. This makes the research significant for both ecological and agricultural management from a theoretical and practical perspective. A gas chromatography-mass spectrometry (GC-MS) system was applied to detect the types and concentrations of PAEs in soil samples while employing 16S rRNA MiSeq high-throughput sequencing technology to explore the structure of soil bacterial communities. By systematically assessing the relationship between the long-term agricultural film mulching soils PAEs pollution status and soil physical and chemical properties, soil enzyme activity and bacterial community structure, this research will reveal the potential accumulation dynamics of PAEs in long-term agricultural activities and their profound impacts on soil ecosystems. This study will provide important empirical evidence to fill the gap of existing short-term simulation studies and provide scientific support for the ecological risk assessment of PAEs and sustainable agricultural management.

2. Materials and methods

2.1. Overview of sampling sites

Soil samples were collected from the main cotton-producing area in Wu{jiaqu} City, located in the Xinjiang Uygur Autonomous of north-western China (87.28°E , 43.98°N) (Fig. 1A). This region experiences low rainfall, significant temperature fluctuations ($\sim 50^\circ\text{C}$), and high evaporation rates ($\sim 2141 \text{ mm}$). The area receives approximately 2850 h of sunshine annually, with an average annual precipitation of 176 mm. Cotton is the primary economic crop in this region, and the main cultivation methods include agricultural plastic film mulching and drip irrigation under mulch (Jiang et al., 2021). Over the past 30 years, the use of agricultural films has expanded significantly, with the annual planting area of agricultural film-mulched cotton reaching up to 8000 ha (Fig. 1B). The average agricultural film residue in the soil is approximately $275.63 \text{ kg hm}^{-2}$, which far exceeds the permissible limits for agricultural film residues established in China (Hu et al., 2019).

2.2. Soil sample collection

In this research, soil samples were collected from sites with mulching durations of 0 (no film), 3, 8, 12, 15, 20, 25, and 30 years, all located within a continuous cotton production area that has utilized the same crop management system for over 30 years. The durations were verified through long-term field records, remote sensing, and interviews with local farmers and agricultural technicians. All fields shared similar conditions regarding soil type (gray desert soil), irrigation method (drip irrigation under mulch), crop variety (cotton), and fertilization practices. No significant land use changes were observed during the study period, ensuring that the duration of plastic film mulching was the primary influencing variable among the sites. Detailed information on the sampling sites is provided in Table S1. For the sampling process, each mulching duration included three adjacent fields, resulting in a total of 24 sampling sites. A systematic sampling strategy was implemented, establishing 9 sampling points per hectare. At each sampling point, five subsamples were randomly collected from the surface soil layers (0–20 cm). After removing fine roots and visible organic debris, these subsamples were thoroughly mixed to create composite samples. This process yielded a total of 72 individual soil samples, which effectively captured variability within each field. Detailed methodologies for

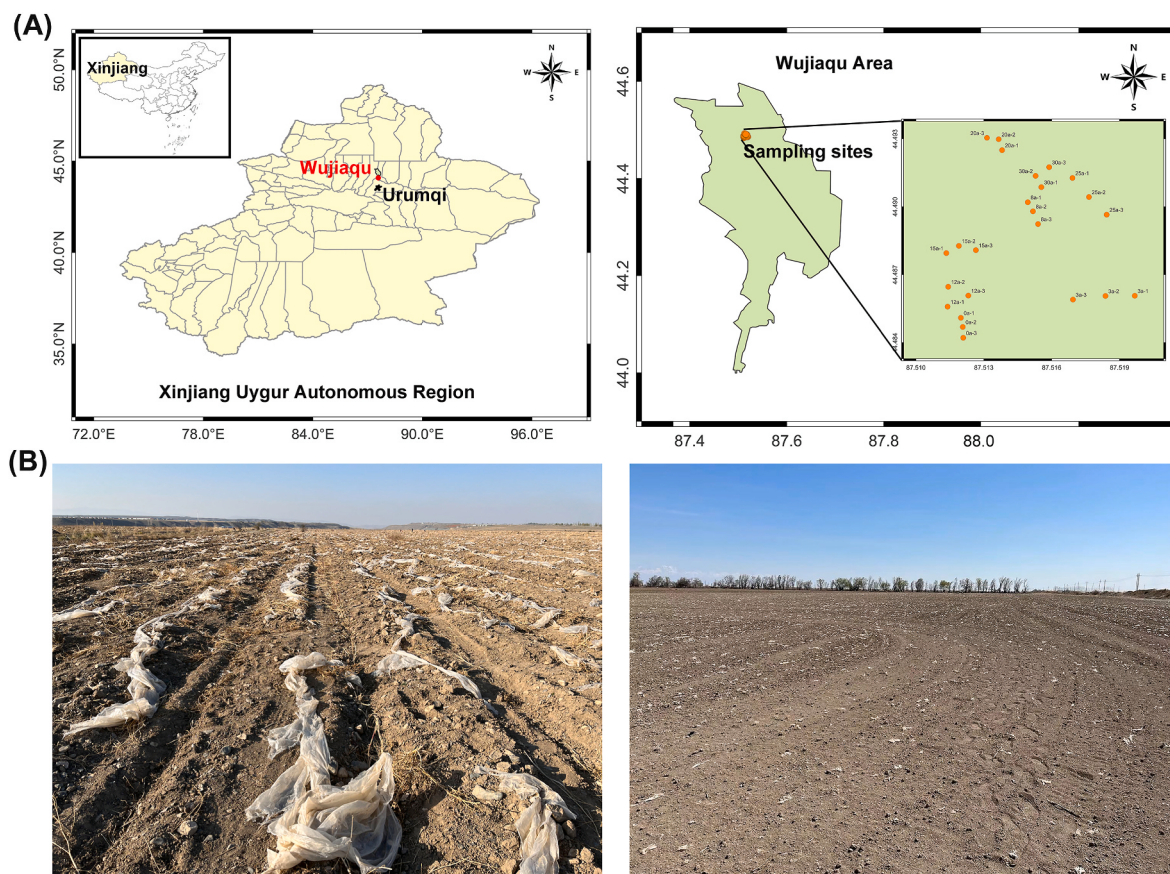


Fig. 1. (A) Schematic map for geographical location and sampling points distribution, and (B) typical view of sampling sites in cotton cropland in Wujaqu, Xinjiang.

soil residual PAEs analysis and soil physicochemical properties analysis is provided in supplementary materials.

2.3. Soil residual PAEs extraction and analysis

Residual PAEs in agricultural film-mulched soil were extracted and determined according to the method described by Alkan et al. (2021).

2.3.1. PAEs extraction

Accelerated solvent extraction was performed on 10 g of cold-dried and ground soil samples using a solvent mixture of acetone/n-hexane (1:1, v/v). The extracts were concentrated using a rotary evaporator (RV10, IKA, Germany) to less than 2 mL, passed through a silica gel solid-phase extraction (SPE) column (1000 mg/6 mL, HOONPO, China), and eluted with 40 mL of acetone/n-hexane (1:3, v/v). The eluate was further concentrated, reconstituted with n-hexane, and brought to a final volume of 1 mL under nitrogen purging. The samples were analyzed by gas chromatography-tandem mass spectrometry (GC-MS/MS).

2.3.2. PAEs quantification

An Agilent 7893B gas chromatography-5975C triple quadrupole mass spectrometry system (Agilent, USA) equipped with a DB-5MS capillary column (30 m length, 0.25 mm inner diameter, 0.25 μ m film thickness) was used. Helium was used as the carrier gas (purity >99.999 %), and the injection volume was 1 μ L. The inlet temperature was set to 290 °C. The temperature program was as follows: initial column temperature of 80 °C (held for 2 min), ramped at 20 °C/min to 180 °C (held for 5 min), followed by a ramp of 5 °C/min to 290 °C (held for 2 min). The electron ionization (EI) source voltage and temperature were set to 70 eV and 230 °C, respectively. All analyses were conducted in selected

ion monitoring (SIM) mode.

2.3.3. Detection limits and quality control

All reagents used in the experiments were chromatographically pure. Glassware was cleaned by heating and ultrasonic cleaning for 1 h, followed by rinsing with distilled water and drying in a muffle furnace at 450 °C for over 6 h prior to use. A procedural blank was included for every 20 samples, and a duplicate sample were assigned for each batch of 10 samples to ensure data reliability. Duplicate samples and procedural blanks followed the same procedures mentioned above and the final statistical results were corrected using blank samples. The calibration was standardized using a five-point calibration curve based on standard mixtures. To ensure the reliability of the experimental method, spiked recovery experiments were conducted using PAE standards before the formal experiments. The results indicated the calibration curves of 6 PAEs had a good linear relationship at the concentration from 0.1 to 5.00 mg L⁻¹. The square of regression coefficient (R^2) ranged from 0.9997 to 0.9999. The method recovery rate, instrumental detection limits (based on three times the signal-to-noise ratio), and method detection limits for the PAEs are listed in Table S2.

2.4. Soil microbial metabolic activity analysis

Soil microbial metabolic activity was analyzed using Biological Eco MicroPlates (BIOLOG, Hayward, USA). Each 96-well MicroPlate contained 31 different carbon sources and a water control, grouped into 6 substrate classes: carbohydrates, amino acids, carboxylic acids, polymers, amines, and phenolic compounds. Briefly, 10 g of soil samples were suspended in 100 mL of sterile normal saline (0.85 %, m/v) and agitated for 30 min at 200 rpm. After settling for 15 min, the soil suspensions were serially diluted to 1:1000. A 150 μ L aliquot of the dilution

was inoculated into each well of the 96-well MicroPlate. The plates were incubated at 25 °C in the dark, and absorbance at 590 nm was recorded every 24 h using an automated microplate reader (PERLONG, China).

Absorbance values were corrected by subtracting the control values and standardized using the following formula to calculate the average well color development (AWCD), which indicates the carbon source utilization capacity of soil microorganisms (Wang et al., 2025).

$$AWCD = \frac{\sum (A_i - A_0)}{N}$$

where A_i is the absorbance value of each well with carbon sources, A_0 refers to the absorbance value of the control group, and N is the number of carbon sources.

2.5. DNA extraction and 16S amplicon sequencing

Total genomic DNA was extracted from soil samples using the Fast DNA Spin Kit for Soils (MP bio, USA) following the manufacturer's guidelines. The quality of the extracted DNA was confirmed by 1 % agarose gel electrophoresis, and the final concentration was measured using a NanoDrop™ One microvolume UV–Vis spectrophotometer (Thermo Fisher Scientific, USA).

The V3-V4 hypervariable region of the bacterial 16S rRNA gene was amplified by polymerase chain reaction (PCR) using universal primers 338F (5'-ACTCCTACGGGAGGCAGCAG-3') and 806R (5'-GGA CTACHVGGGTWTCTAAAT-3'). The PCR conditions included an initial denaturation at 98 °C for 1 min, followed by 30 cycles of denaturation at 98 °C for 10 s, annealing at 50 °C for 30 s, and elongation at 72 °C for 30 s, with a final elongation at 72 °C for 5 min. PCR products were further purified using 2 % agarose gel and TIANgel Midi Purification Kit (TIANGEN Biotech, Beijing, China). The resulting amplicons were sequenced on the Illumina MiSeq platform by Novogene Biotech Co., Ltd (Beijing, China).

After sequencing, paired-end reads were assigned to samples based on unique barcodes and truncated by removing the barcode and primer sequence. Paired-end reads were merged using FLASH (V1.2.7) to obtain raw tags. Quality filtering was performed to remove adapter sequences and low-quality reads, yielding high-quality clean tags using SOAP (v1.7.0). Chimera sequences were removed, and the remaining effective tags were denoised using QIIME2 software (Version QIIME2-202006), generating initial Amplicon Sequence Variants (ASVs) for species annotation. ASVs were classified at 97 % similarity, and those with only a single sequence were excluded before further analysis. Taxonomic identification of ASVs was conducted against the 16S/Silva/v138 bacterial sequence database. The sequences are available in GenBank at <https://www.ncbi.nlm.nih.gov/sra/PRJNA1164426>, with BioSample SAMN43901167 and BioProject ID PRJNA1164426.

While 16S rRNA sequencing primarily provides insights into the taxonomic composition of microbial communities, it can also inform on their functional potential through prediction tools like the Functional Annotation of Prokaryotic Taxa (FAPROTAX) (Louca et al., 2016). FAPROTAX predicts functional profiles based on 16S rRNA gene sequences utilizing an extensive annotation library of cultivable bacteria. This tool is particularly useful for predicting functions in environmental samples, especially regarding processes like carbon cycling and nitrogen fixation. However, it is essential to note that functional predictions based solely on 16S data are limited, as they cannot capture the full range of functional genes or metabolic pathways.

2.6. Statistical analysis

All statistical analyses were performed using SPSS (Version 23.0, IBM, New York, USA). One-way analysis of variance (ANOVA) and t-tests were performed to determine the difference between treatments, and the p-value of <0.05 considered statistically significant. Prior to

applying any parametric tests, we confirmed the normality of data distributions using the Shapiro–Wilk test. The results indicated that the assumption of normality was satisfied for the majority of variables. Alpha diversity (Shannon and Chao1 indices) was used to estimate the complexity of microbial communities in different samples. This was calculated using QIIME software (http://qiime.org/scripts/alpha_diversity.html) to assess the richness and evenness of microbial communities and their correlation with environmental variables and PAEs concentration. Pearson correlation analysis was employed for correlation assessments. This analysis helps elucidate the strength and direction of associations between environmental factors, including PAEs and microbial community structure, enhancing our interpretation of the ecological impacts of PAEs. Molecular ecological networks were constructed using the Integrated Network Analysis Pipeline (iNAP, <http://mem.rcees.ac.cn:8081>). Co-occurrence networks of microbial communities from the two sites were visualized in Gephi (version 0.9.5) to explore associations between species and co-occurrence patterns within the core microbiota. Redundancy analysis (RDA) was performed using Canoco (version 5) software to determine the relationships between soil physicochemical properties, residual PAEs concentrations, and all bacterial ASVs. Effect sizes RDA results were included to provide a comprehensive understanding of the correlations between PAEs and microbial communities. This ordination method was selected due to the gradient length of the axis (2.98 < 3.0), which is suitable for linear modeling of species-environment relationships. Important data exported from Canoco into R 4.2.2 and use the 'vegan' package to plot an RDA diagram showing 95 % confidence intervals. The functional profile of bacterial communities was predicted using the FAPROTAX database, a comprehensive cultivable bacterial annotation library, based on 16S rRNA gene sequences (www.zoology.ubc.ca/louca/FAPROTAX). Origin 9 (OriginLab Inc., USA) was used to draw box plots. ArcGIS 10.2 was used to draw a map of sampling sites.

3. Results

3.1. Accumulation of PAEs and soil physiochemical properties

Following the application of agricultural film mulching in cotton fields, six types of PAEs, namely DMP, DEP, DBP, BBP, DEHP, and DnOP, were found to migrate from the plastic film into the surrounding soil. The concentration changes of total and individual PAEs are presented in Table 1. The total PAEs (ΣPAEs) concentration in the soil under agricultural film mulching was significantly higher than that in open-field soil (0a), with cumulative concentration ranging from 2.43 to 6.40 mg/kg. As the duration of agricultural film use increased, ΣPAEs concentrations peaked at 8 years of mulching before gradually decreasing. Among the detected PAEs, DEHP was the predominant compound, with the highest concentration of 2.24 ± 0.11 mg/kg (8a), followed by DBP (1.79 ± 0.06 mg/kg) (8a), DnOP (1.26 ± 0.13 mg/kg) (12a), BBP (0.67 ± 0.02 mg/kg) (8a), DMP (0.52 ± 0.02 mg/kg) (8a), and DEP (0.27 ± 0.02 mg/kg) (8a). Most PAEs reached their peak concentrations in the 8th year of mulching, except for DnOP. Although extending the use of agricultural film reduced the concentrations of all PAEs, significant residues remained in the soil. DMP and DEP had minimal residues (~0.1 mg/kg), while DEHP and DnOP exhibited higher residues (~1.0 mg/kg), indicating a more obvious environmental impact from DEHP and DnOP.

Long-term agricultural film mulching significantly influences the physicochemical properties of agricultural soil. As shown in Table 2, all soil samples exhibited weak alkalinity. Over the period of 8–12 years of agricultural film mulching, the pH slightly decreased from 8.24 (0a) to 7.85 (12a), but subsequently recovered to its original value. However, more notable changes were observed in the nutrient structure of the soil ecosystem, with most concentrations increasing compared to 0a. The organic matter (OM) content significantly increased and fluctuated around 15.00 g/kg in all agricultural film-mulched soils. Both ammonium nitrogen (AN) and available phosphorus (AP) content exhibited an

Table 1

Concentration of PAEs in cotton fields with different years of film mulching.

| Samples | Concentrations of PAEs (mg/kg) | | | | | | Σ PAEs |
|---------|--------------------------------|---------------|--------------|--------------|--------------|----------------|---------------|
| | DMP | DEP | DBP | BBP | DEHP | DnOP | |
| 0a | 0.00 ± 0.00e | 0.03 ± 0.01f | 0.11 ± 0.01e | 0.11 ± 0.02c | 0.18 ± 0.13e | 0.32 ± 0.05d | 0.75 ± 0.09f |
| 3a | 0.12 ± 0.02b | 0.18 ± 0.02b | 1.59 ± 0.10b | 0.59 ± 0.10b | 0.60 ± 0.07d | 0.42 ± 0.04d | 3.49 ± 0.11bc |
| 8a | 0.52 ± 0.02a | 0.27 ± 0.02a | 1.79 ± 0.06a | 0.67 ± 0.02a | 2.24 ± 0.11a | 0.91 ± 0.03c | 6.40 ± 0.04a |
| 12a | 0.08 ± 0.01cd | 0.14 ± 0.02c | 0.50 ± 0.03c | 0.57 ± 0.01b | 1.11 ± 0.07b | 1.26 ± 0.13a | 3.65 ± 0.24b |
| 15a | 0.07 ± 0.01d | 0.15 ± 0.01c | 0.47 ± 0.01c | 0.53 ± 0.02b | 1.00 ± 0.06b | 1.15 ± 0.11 ab | 3.37 ± 0.12c |
| 20a | 0.07 ± 0.01d | 0.12 ± 0.03cd | 0.51 ± 0.01c | 0.53 ± 0.01b | 1.04 ± 0.02b | 1.05 ± 0.03b | 3.31 ± 0.06c |
| 25a | 0.07 ± 0.01d | 0.07 ± 0.01e | 0.25 ± 0.01d | 0.53 ± 0.01b | 0.87 ± 0.01c | 1.07 ± 0.01b | 2.86 ± 0.01d |
| 30a | 0.09 ± 0.02c | 0.11 ± 0.01d | 0.23 ± 0.03d | 0.09 ± 0.01c | 0.86 ± 0.01c | 1.06 ± 0.02b | 2.43 ± 0.02e |

Note: Values in the table are expressed as mean ± standard deviation ($n = 3$), and different letters appearing in each row indicate significant differences between samples ($p < 0.05$). There were no significant differences between values followed by the same letters in the same row. 0a, 3a, 8a, 12a, 15a, 20a, 25a, and 30a referred to the soil samples mulched with plastic film in different years.

Table 2

Physicochemical properties in cotton fields with different years of film mulching.

| Samples | Soil nutrition content | | | | | |
|---------|--------------------------|----------------|----------------|------------------|---------------|----------------|
| | OM (g·kg ⁻¹) | AN (mg/kg) | AP (mg/kg) | AK (mg/kg) | TWS (g/kg) | pH |
| 0a | 9.27 ± 0.91c | 20.17 ± 1.10f | 4.77 ± 1.59a | 314.17 ± 5.18e | 8.50 ± 0.46a | 8.24 ± 0.11b |
| 3a | 17.50 ± 2.23a | 48.80 ± 1.44e | 7.00 ± 1.59bc | 998.07 ± 72.10a | 3.37 ± 1.33bc | 8.47 ± 0.06a |
| 8a | 15.50 ± 0.78 ab | 49.57 ± 7.40e | 6.13 ± 0.57c | 447.53 ± 10.70c | 3.60 ± 0.76b | 7.90 ± 0.09c |
| 12a | 13.57 ± 1.10b | 62.07 ± 4.80d | 5.03 ± 0.23c | 374.43 ± 15.70d | 8.93 ± 1.65a | 7.85 ± 0.03c |
| 15a | 17.07 ± 1.75a | 89.77 ± 5.60b | 9.47 ± 0.93 ab | 496.73 ± 52.79bc | 1.97 ± 0.31cd | 8.10 ± 0.12b |
| 20a | 14.87 ± 1.31 ab | 77.87 ± 7.36c | 11.07 ± 2.77a | 529.80 ± 7.00b | 1.93 ± 0.47cd | 8.27 ± 0.11b |
| 25a | 16.00 ± 1.21 ab | 100.17 ± 2.41a | 11.80 ± 2.81a | 550.60 ± 21.26b | 0.57 ± 0.25d | 8.13 ± 0.16b |
| 30a | 17.13 ± 1.42a | 76.90 ± 0.40c | 10.90 ± 1.01a | 501.37 ± 12.62bc | 0.83 ± 0.06d | 8.31 ± 0.14 ab |

Note: Values in the table are expressed as mean ± standard deviation ($n = 3$), and different letters appearing in each row indicate significant differences between samples ($p < 0.05$). There were no significant differences between values followed by the same letters in the same row.

upward trend over time. In contrast, available potassium (AK) content rose sharply from 314.17 ± 5.18 mg/kg (0a) to 998.07 ± 72.00 mg/kg (3a), but then significantly decreased and stabilized in subsequent years. Additionally, the total water-soluble (TWS) concentrations showed a nonmonotonic decrease as the duration of agricultural film mulching increased.

3.2. Soil enzyme activity

The findings presented above indicate that long-term agricultural film mulching significantly impacts soil nutrients. To further explore this, we investigated changes in the enzymatic activities of catalase and alkaline phosphatase in the soil. As shown in Fig. 2A and B, compared to control soil (0a), there were significant increases in the activities of

catalase ($p = 0.0005$), alkaline phosphatase ($p = 0.0001$), during the 3rd (3a) and 8th (8a) years of agricultural film mulching. For example, after 3 years of mulching, the activities of alkaline phosphatase increased nearly tenfold. Initially, extending the duration of mulching initially resulted in a decrease in enzyme activity, followed by an increase, which was consistent with changes in PAEs concentration levels.

3.3. Soil microbial metabolic activity

Average well color development (AWCD) was used to reflect carbon source utilization patterns and quantify soil microbial metabolic activity, with higher AWCD values indicating stronger metabolic activity (Wang et al., 2022a). The dynamic changes in AWCD values for different soil samples were measured every 24 h (Fig. 3A). Overall, AWCD

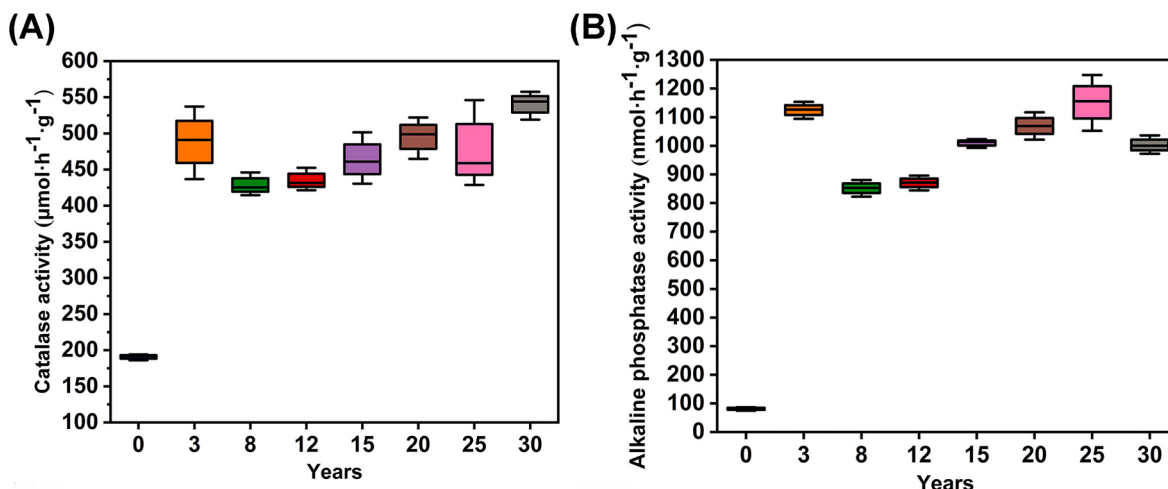


Fig. 2. (A) Catalase, (B) alkaline phosphatase activities in open field soil (0a) and agricultural film mulched soil with different years.

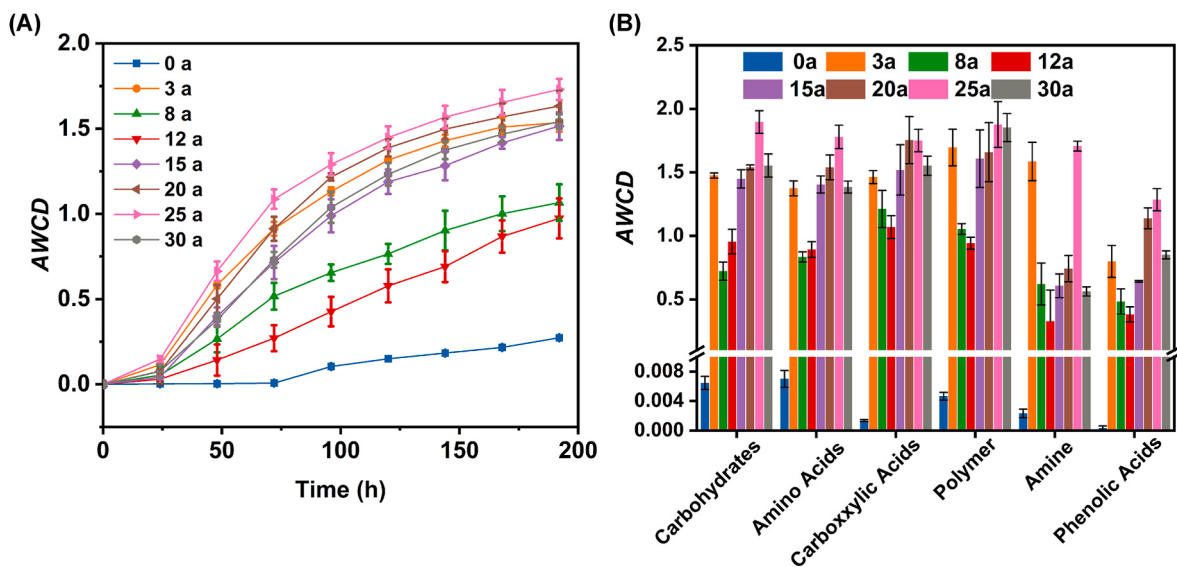


Fig. 3. (A) The dynamic changes of average well color development (AWCD) over cultivation time and (B) utilization of soil microbial community to 6 carbon substrates in cotton fields with different years of film mulching.

showed an increasing trend as cultivation time extended. No significant changes in AWCD were observed during the first 24 h, but between 24 and 144 h (with 0a between 72 and 192 h), there was a rapid increase in AWCD, indicating robust microbial activity. After 168 h, the growth rate of AWCD slowed down and tended to stabilize, likely due to reduced microbial activity in the soils. These results demonstrated that agricultural film mulching significantly enhanced the carbon source utilization by soil microorganisms, although effects varied depending on the duration of mulching. The lowest AWCD value was recorded in open field soil (0a), while a marked increase was observed in the 3rd year of agricultural film mulching (3a). This was followed by a significant decrease in the 8th and 12th years. Fields with histories of 20 (20a) and 25 years (25a) of agricultural film mulching exhibited generally higher AWCD values, suggesting that more microorganisms developed the capacity to metabolize organic substrates in the Biological Eco MicroPlates.

Based on the AWCD results, the ability of soil microorganisms to utilize 6 carbon sources was further investigated to analyze the metabolic activities of the bacterial community, including carbohydrates, amino acids, carboxylic acids, polymers, amines, and phenolic acids. Overall, agricultural film mulching significantly enhanced the ability of soil microorganisms to utilize various carbon sources (Fig. 3B). The bacterial community exhibited relatively higher utilization capacities for carbohydrates, amino acids, carboxylic acids, and polymers compared to other substrates. As the duration of agricultural film mulching increased, the utilization capacity of soil microorganisms for all carbon sources initially rose, followed by a decrease and another increase, consistent with the dynamic changes in soil enzyme activity. Notably, a significant enhancement in the utilization of all carbon sources was observed in the 3rd year (3a). Specifically, soil microorganisms in the 25th year (25a) of agricultural film mulching exhibited the highest capacity for carbon source utilization. These results indicate that agricultural film mulching can alter the soil ecological environment by affecting microbial metabolism.

3.4. Bacterial community analysis through amplicon sequencing

3.4.1. Overview of sequencing data

The effect of agricultural film residue on bacterial community diversity was assessed across different years of agricultural film mulching using 16S rDNA amplicon sequencing. The sequencing results are summarized in Table S3. A total of 9,735,351 paired reads were generated

from 72 samples. After filtering out short and low-quality reads, singletons, replicates, and chimeras, 7,748,245 high-quality effective tags were obtained. The average length of these effective tags ranged from 414.90 to 424.06 bp, with a Q20 value exceeding 98 %. Based on the evaluation of sequencing quality through GC content and Q30, all parameters met the requirements for subsequent analysis.

The sequences were finally clustered into 6,893,059 amplicon sequence variants (ASVs) at a 97 % sequence identity threshold. These ASVs were relatively evenly distributed across the samples, ranging from 734,968 to 927,949. The rarefaction curves of bacterial sequences (Fig. S1) approached a plateau after reaching 20,000 sequences, indicating comprehensive coverage of taxonomic diversity. Analysis of the representative sequences of ASVs using the Bayesian algorithm of RDP classifier identified a total of 1 domain, 2 kingdoms, 54 phyla, 146 classes, 366 orders, 624 families, 1373 genera, and 806 species. Therefore, we conclude that the sequencing depth and data volume are sufficient to accurately reflect the bacterial community composition and structure in each soil sample.

3.4.2. Soil bacterial community diversity

The characteristics of the bacterial community were reflected in species diversity and relative abundance, indicating the community complexity and composition of the soil samples. The α -diversity indices, including the Shannon and Chao 1 indexes, were used to evaluate bacterial community diversity in cotton field soils with different years of agricultural film mulching. As shown in Fig. 4A and B, agricultural film application significantly impacted bacterial diversity. In the 3rd and 8th years of agricultural film mulching, both Shannon and Chao 1 indexes increased compared to open field soil (0a), indicating higher species richness (Chao 1) and diversity (Shannon) due to agricultural film residues. However, no significant change in α -diversity was observed in subsequent years of mulching. Besides, principal coordinate analysis (PCoA) and non-metric multidimensional scaling (NMDS) were conducted to visualize dissimilarities among bacterial communities at the ASV level. As shown in Fig. 4C, the ASV abundance in the 0a group was clearly separated from other groups, indicating distinct community structures. In contrast, agricultural film-mulched groups exhibited varying degrees of overlap. The first principal axis (PCoA1 = 23.76 %) and second principal axis (PCoA2 = 10.04 %) explained a total variation of 33.80 % in bacterial community composition. NMDS analysis using weighted Bray-Curtis distances (Fig. 4D) further reflected the separation pattern among bacterial communities. Significant separation was

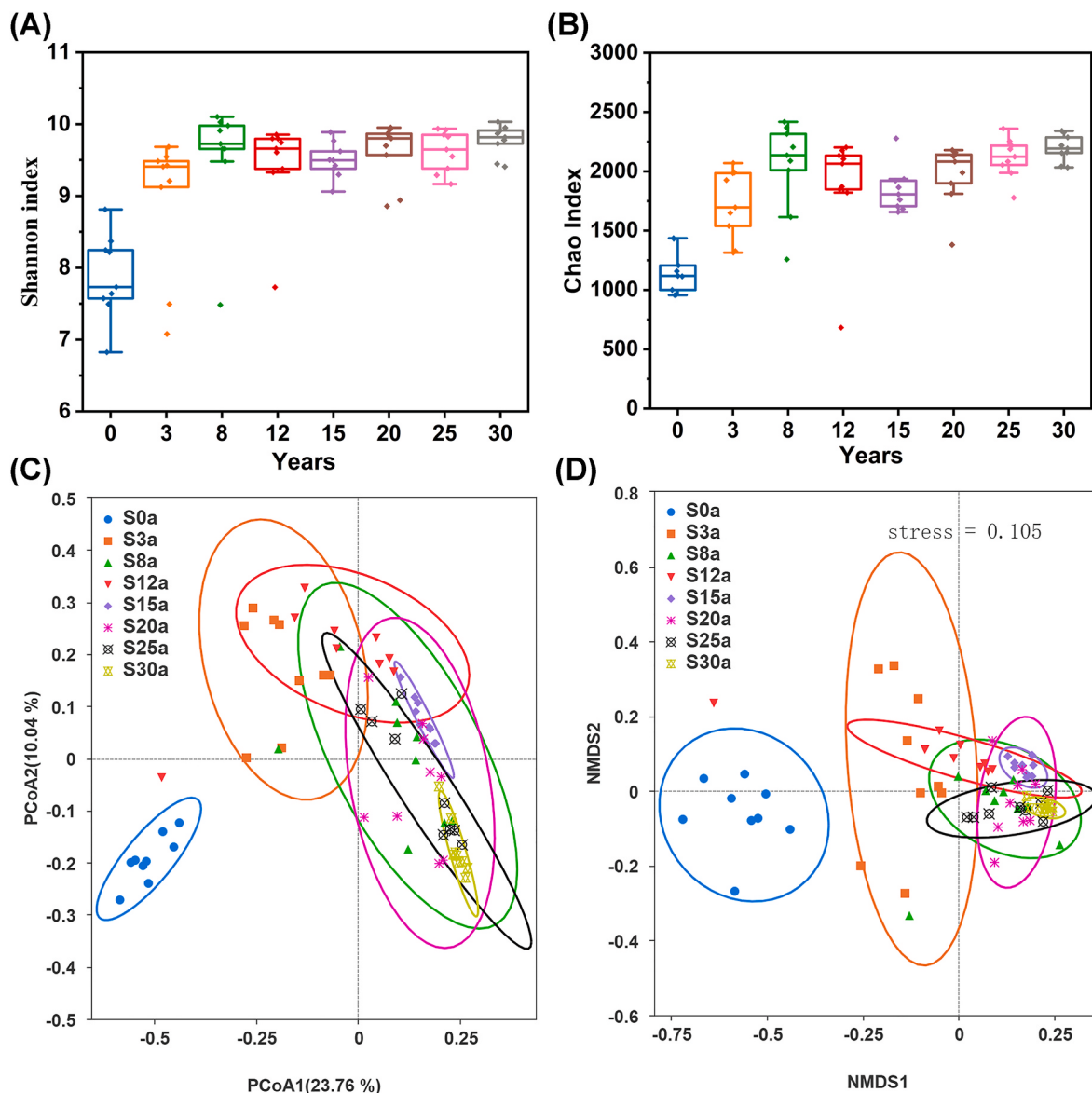


Fig. 4. (A) Shannon, (B) Chao, (C) PCoA, and (D) NMDS in open field soil (0a) and agricultural film mulched soil with different years.

observed among the bacterial communities of 0a, 3a, and 8a samples, while strong clustering occurred in samples after 12 years of agricultural film mulching. Additionally, ANOSIM analysis confirmed significant differences in bacterial community structure among soils mulched with agricultural film ($R = 0.673$, $P < 0.001$) (Fig. S2). These findings indicate that agricultural film residues significantly altered the soil bacterial community.

3.4.3. Bacterial community composition and structure

The bacterial community composition across different soil samples was analyzed at both the phylum and genus levels. The results showed similar taxonomic compositions in all soil samples (Fig. 5). A total of 41 phyla and 802 genera were identified, with an average relative abundance exceeding 1 % for 9 phyla and 15 genera. The bacterial composition at the phylum level was consistent across all groups, with the most dominant phyla being Proteobacteria (25.40 %), Actinobacteriota (20.84 %), Bacteroidota (15.37 %), Gemmatimonadota (13.44 %), Acidobacteriota (8.61 %), Chloroflexi (3.85 %), Firmicutes (3.81 %), Verrucomicrobiota (1.87 %), and Myxococcota (1.69 %). Significant differences were observed between open field soil (0a) and agricultural film-mulched soil. Compared to 0a, agricultural film mulching

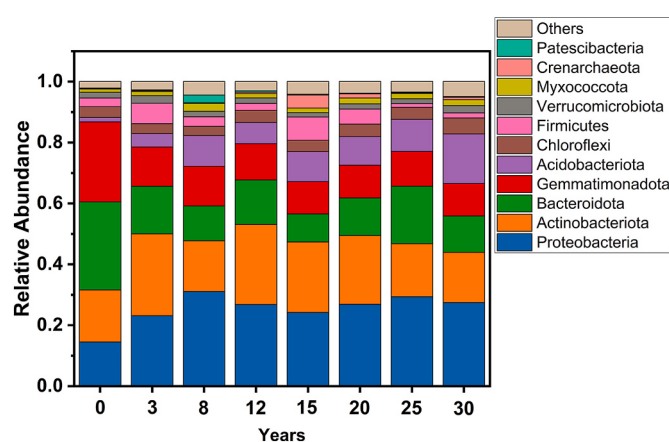


Fig. 5. Relative abundance of soil bacteria at phylum level.

significantly enhanced the relative abundances of Proteobacteria, Actinobacteriota, and Acidobacteriota, while decreasing the relative abundances of Bacteroidota and Gemmatimonadota after 3 or 8 years of mulching. At the genus level, the most dominant genera included *S0134_terrrestrial_group* (3.52 %), *Vicinamibacteraceae* (3.10 %), *Pedobacter* (2.23 %), *Massilia* (2.13 %), *Spingomonas* (1.97 %), *Adhaeribacter* (1.53 %), *Pseudomonas* (1.37 %), *Pseudarthrobacter* (1.35 %), *Skermanella* (1.27 %), *Pontibacter* (1.21 %), *Gemmatimonas* (1.15 %), *0319-7L14* (1.13 %), *Rubrobacter* (1.06 %), *Pedosphaeraceae* (1.05 %), and *RB41* (1.01 %) (Fig. S3). The unclassified *S0134_terrrestrial_group* from the Gemmatimonadota phylum and *Rubrobacter* from the Actinobacteria phylum were more abundant in open field soil (0a) but significantly decreased after agricultural film mulching, especially between the 15th and 30th years of mulching. A general trend observed was that the abundance of other dominant genera initially increased, then decreased, and finally increased again as the duration of agricultural film mulching progressed. These results indicate that the richness and composition of bacterial communities in agricultural film mulched-soil are significantly influenced by the duration of mulching.

The nonparametric factorial Kruskal-Wallis sum-rank test was applied to screen bacterial biomarkers in open field soil and agricultural film-mulched soil by comparing differences in bacteria taxa, with a linear discriminant analysis (LDA) score threshold of 4. A total of 32 (0a vs 3a), 47 (0a vs 8a), 39 (0a vs 12a), 61 (0a vs 15a), 45 (0a vs 20a), 43 (0a vs 25a) and 55 (0a vs 30a) biomarkers were identified with significantly different abundances between the 0a group and each agricultural film-mulched group. Among them, 24 shared biomarkers were found across all groups. Of the shared biomarkers, 8 were significantly enriched in all agricultural film-mulched soil samples ($p < 0.05$) (Fig. 6A), including Acidobacteriota (phylum), Proteobacteria (phylum), Alphaproteobacteria (class), Gemmatimonadetes (class), Vicinamibacteria (class), Gemmatimonadaceae (family), Gemmatimonadales (order), Vicinamibacteriales (order), which belong to the phyla Acidobacteriota, Gemmatimonadota, and Proteobacteria. In contrast, 16 biomarkers were enriched in open field soil (Fig. 6B), such as BD2_11_terrrestrial_group (class), Balneolales (order) and Rhodothermaceae (family), which were associated with the phyla Bacteroidota and Gemmatimonadota. These results demonstrate that the shared

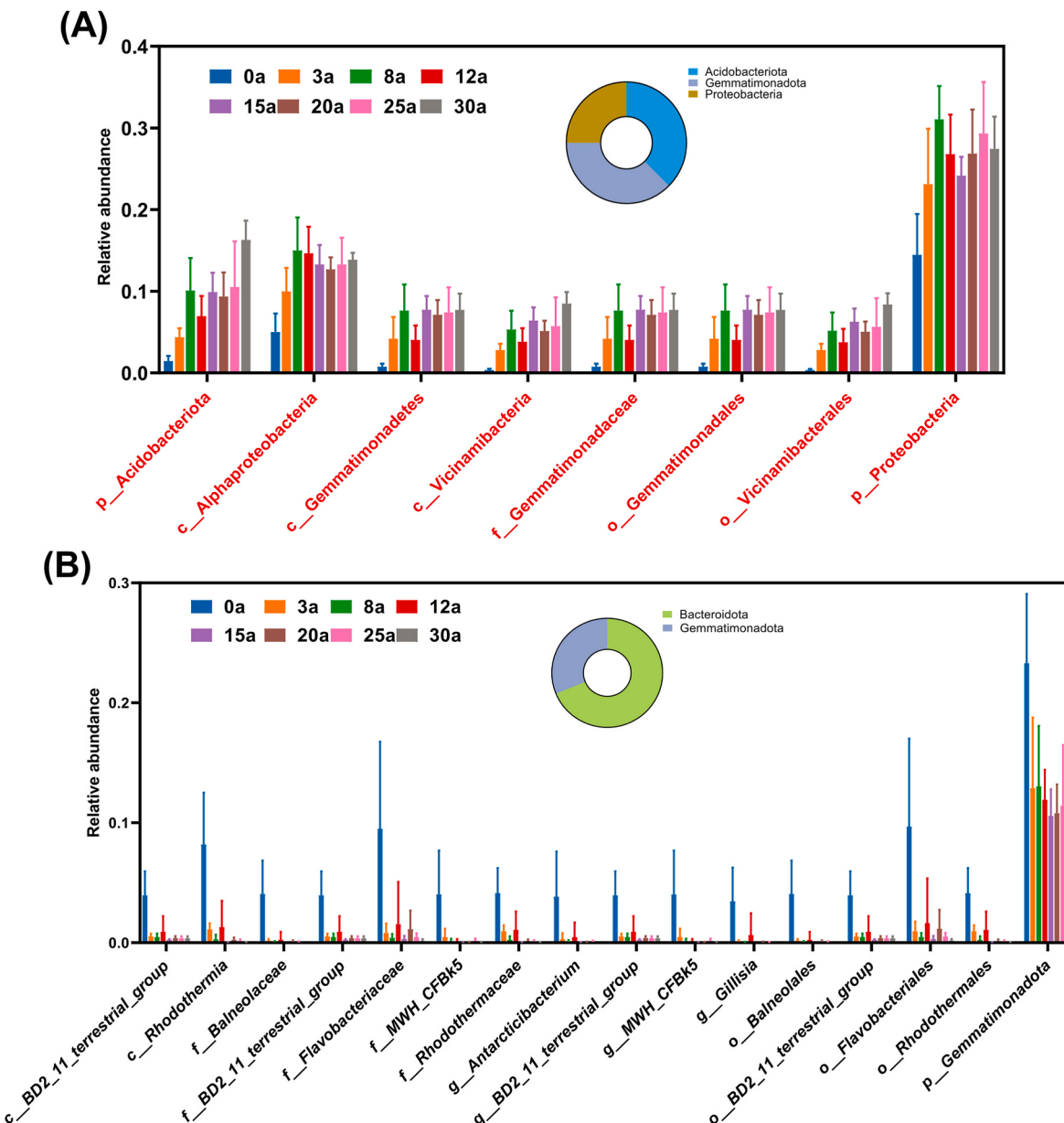


Fig. 6. (A) Shared biomarkers enriched in soil samples of cotton fields with film mulching (red color) and (B) enriched in soil samples of open field (black color).

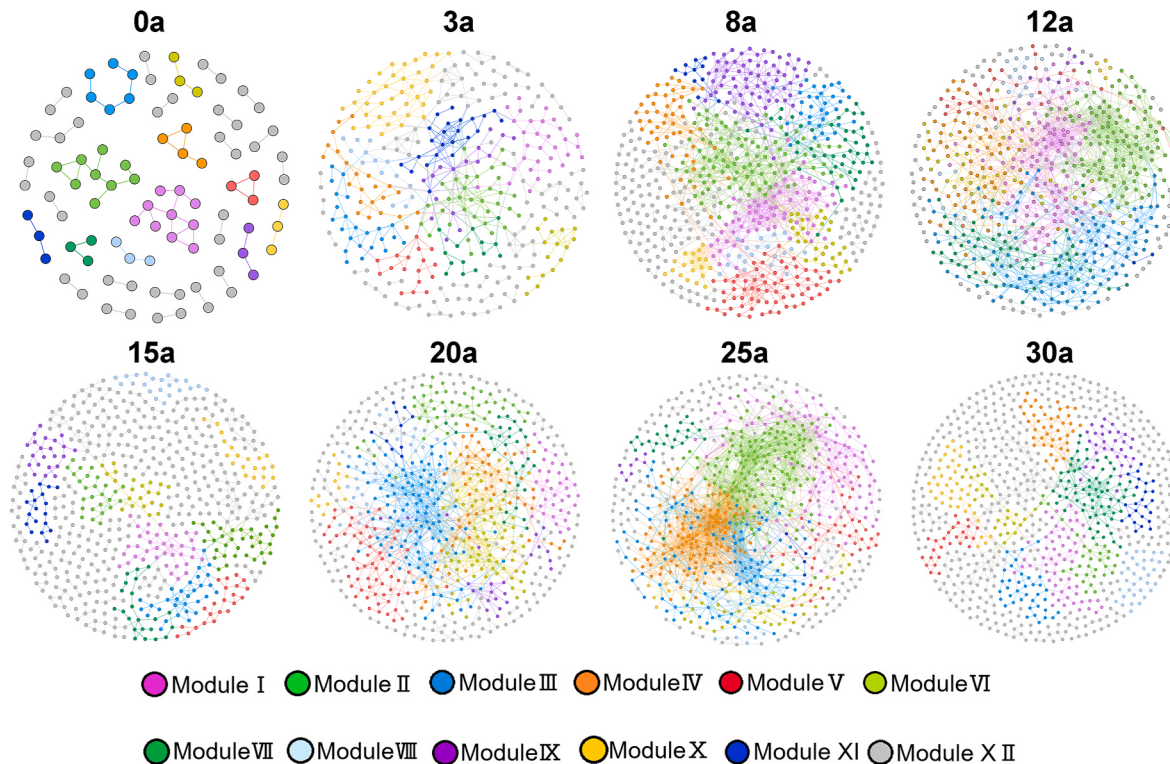
biomarker microbial communities exhibit a degree of stability, indicating good adaptability and resilience to different environmental stresses.

3.4.4. Bacterial community co-occurrence network analysis

Co-occurrence networks based on Spearman correlations among ASVs were constructed to analyze the effects of long-term agricultural film mulching on soil bacterial community associations. The topological properties of these networks were calculated to identify differences among samples. As shown in Fig. 7, bacterial networks in agricultural film-mulched soil were distinct from those in open field soil and varied across different mulching years. The topology parameters of the bacterial networks were further analyzed. In open field soil (0a), the networks consisted of 91 nodes and 65 edges. In contrast, networks after 3, 8, and 12 years of agricultural film mulching contained 358 nodes and 515 edges, 670 nodes and 1487 edges, and 613 nodes and 1885 edges, respectively, indicating a more complex network in agricultural film-mulched soil. Notably, the topology parameters obviously decreased in the 15th year of agricultural film mulching (613 nodes and 671 edges), but increased again in subsequent years, reaching their highest network complexity in the 25th year (747 nodes and 2956 edges). Additionally, the effects of agricultural film mulching on the average

degree and average clustering coefficient mirrored the trends observed in the number of nodes and edges. Collectively, these findings suggest that the application of agricultural film in cotton fields enhanced bacterial network complexity, with notable differences associated with varying mulching durations.

Keystone species play a crucial role in shaping the network structure of bacterial communities. Therefore, keystone species were identified in agricultural film-mulched soil based on their within-module connectivity (Z_i) and among-module connectivity (P_i). The results revealed a total of 124 keystone nodes across all agricultural film-mulched soil networks. In contrast, all nodes in the open soil (0a) network were classified as peripherals, meaning they had links only within their own modules. Similar to the topological properties, the number of keystone nodes also showed an initial increase, followed by a decrease, and then increased again after long-term mulching with agricultural film. Specially, the following numbers of keystone species were observed in each network: 6 in the 3a network (1 module hub, 4 connectors, and 1 network hub), 18 in the 8a network (8 module hubs and 10 connectors), 20 in the 12a network (10 module hubs and 10 connectors), 13 in the 15a network (8 module hubs and 5 connectors), 19 in the 20a network (6 module hubs and 13 connectors), 33 in the 25a network (12 module hubs and 21 connectors), and 15 in the 30a network (12 module hubs and 15 connectors).



Co-occurrence network topology parameters

| | S0a | S3a | S8a | S12a | S15a | S20a | S25a | S30a |
|---|------|-------|-------|-------|-------|-------|-------|-------|
| Total nodes | 91 | 358 | 670 | 613 | 613 | 661 | 747 | 823 |
| Total links | 65 | 515 | 1487 | 1885 | 671 | 1272 | 2956 | 1021 |
| R square of power-law | 0.99 | 0.94 | 0.94 | 0.91 | 0.89 | 0.95 | 0.97 | 0.92 |
| Average degree (avgK) | 1.43 | 2.88 | 4.44 | 6.15 | 2.19 | 3.85 | 7.91 | 2.48 |
| Average clustering coefficient (avgCC) | 0.11 | 0.22 | 0.25 | 0.29 | 0.15 | 0.21 | 0.27 | 0.16 |
| Net.Diamet | 5.00 | 20.00 | 19.00 | 17.00 | 33.00 | 20.00 | 23.00 | 26.00 |

Fig. 7. Co-occurrence network and topology parameters of soil bacterial community with different film mulching years. Networks are constructed at the ASV level. The size of nodes is scaled to the degree of nodes, and they are colored according to different modules.

and 3 connectors). These keystone species belonged to the phyla Acidobacteriota, Actinobacteriota, Bacteroidota, Chloroflexi, Desulfovibacterota, Gemmatimonadota, Myxococcota, and Proteobacteria. Notably, no keystone species were shared across all agricultural film-mulched soil samples, indicating that the network structure may differ at the keystone species level. However, ASV 16 (Actinobacteriota) was shared between the 3a and 8a networks, while ASV469

(Gemmatimonadota) was shared between the 8a and 12a networks. Additionally, ASV11 (Gemmatimonadota), ASV111 (Acidobacteriota), and ASV970 (Desulfovibacterota) in the 12a network, as well as ASV230 (Chloroflexi) and ASV48 (Acidobacteriota) in the 20a network, were shared in the 25a network. These species belonged to the bacterial families Euzebyaceae, Gemmatimonadaceae, S0134_terrrestrial, Vicinamibacteraceae, OLB14, and Pyrinomonadaceae. The findings provide

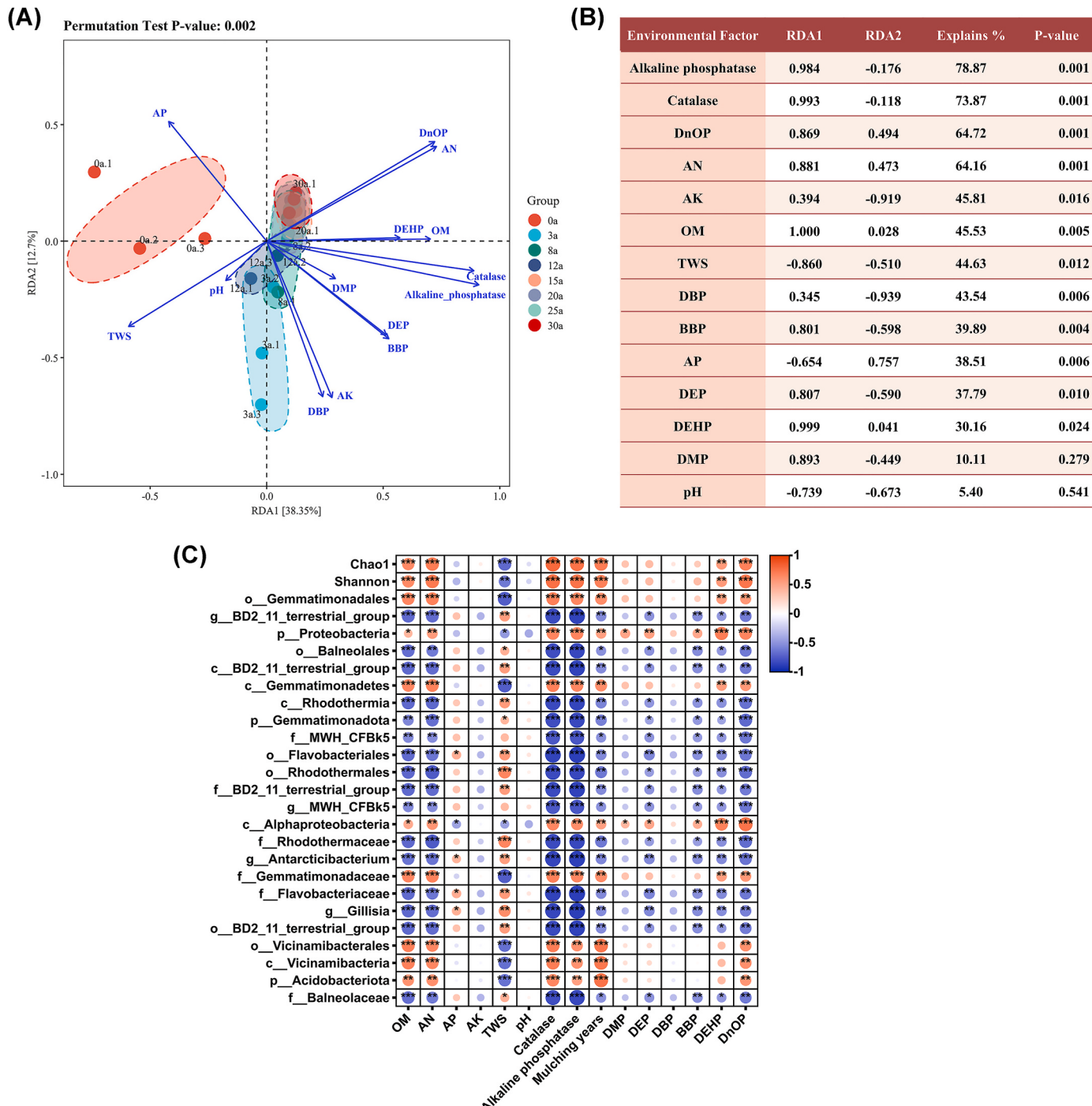


Fig. 8. (A) Correlation analysis and (B) their explanations based on RDA between environmental factors and bacterial community composition in plastic film-mulched soil for different years. The environmental factors and their explanations were shown in the plots. The blue arrows represent the different environmental factors. The length and angle of the arrows represent the degree of influence of soil environmental factors on bacterial community composition and the positive and negative correlation between the two. The acute angle indicates the positive correlation, and the obtuse angle indicates the negative correlation. The different pure color shaded area depict the best-fit trendline and the 95 % confidence interval of the linear regression, respectively. (C) Pearson correlation heat maps of environmental factors with bacterial diversity and biomarkers. Red represents a positive correlation, and blue represents a negative correlation (*P < 0.05; **P < 0.01; ***P < 0.001).

insights into the potential screening of PAEs degrading bacteria.

3.5. Correlation between environmental factor and bacterial community composition

Correlation analysis was performed to evaluate the impact of environmental factors on the bacterial community of agricultural film-mulched soil. After normalizing all bacterial ASVs, redundancy analysis (RDA) in Fig. 8A and B was chosen for correlation analysis due to an axis gradient length of 2.98 (<3.0). The ordination diagram showed that the first two axes of the RDA explained 51.05 % of the total variation in the bacterial community, with 38.35 % attributed to RDA1 and 12.7 % to RDA2. Among the environmental factors, alkaline phosphatase (with an explanation rate of 78.87 %) had the greatest impact on the bacterial community, followed by catalase (73.87 %), DnOP (64.72 %), and AN (64.16 %). Among them, TWS and AP were significantly positively correlated with the bacterial community composition in the 0a sample ($P < 0.05$), while alkaline phosphatase and DnOP showed negative correlations. As the duration of agricultural film mulching increased, the correlations reversed, indicating that these environmental factors significantly influence the bacterial community composition in agricultural film-mulched soil.

Pearson correlation analysis was further applied to investigate the relationships between bacterial diversity, biomarkers, and environmental factors (Fig. 8C). The correlation heatmap revealed that OM, AN, catalase, alkaline phosphatase, years of agricultural film mulching, and DnOP were significantly positively correlated with both the Chao 1 and Shannon indices ($P < 0.001$), while showing a significant negative correlation with TWS ($P < 0.01$, $P < 0.001$). In the agricultural film-mulched cotton fields, the 24 shared biomarkers exhibited significant correlations with OM, AN, TWS, catalase, alkaline phosphatase, and DnOP ($P < 0.05$, $P < 0.01$, $P < 0.001$). Eight biomarkers, enriched with increasing years of mulching, showed a significant positive correlation ($P < 0.01$, $P < 0.001$). These included Acidobacteriota, Alphaproteobacteria, Gemmatimonadetes, Vicanamibacteria, Gemmatimonadaceae, Gemmatimonadales, Vicanamibacterales, and Proteobacteria. Conversely, the 16 shared biomarkers that decreased with increasing mulching years exhibited the opposite correlation trend. Overall, the biomarkers displayed opposite correlation trends based on the duration of agricultural film mulching. TWS also exhibited an inverse correlation with other environmental factors in relation to bacterial diversity and shared biomarkers. Additionally, environmental factors such as AP, AK, pH, DMP, and DBP showed no significant correlations with bacterial diversity or biomarkers.

Further correlation analysis between environmental factors was conducted (Fig. S4), and the results indicated the significant negative correlations between five individual PAEs (DMP, DEP, DBP, BBP, DEHP) and DnOP with AP and pH ($P < 0.05$, $P < 0.01$, $P < 0.001$). The six individual PAEs showed a positive, though not statistically significant, correlation with OM. However, DnOP exhibited a strong positive correlation with AN ($r = 0.65$, $P < 0.001$). In terms of soil enzyme activities, BBP ($r = 0.55$, $P < 0.01$) and DnOP ($r = 0.55$, $P < 0.01$) were strongly positively correlated with alkaline phosphatase, while DnOP also demonstrated a strong positive correlation with catalase ($r = 0.58$, $P < 0.001$). Notably, DnOP content was significantly positively correlated with the number of years of agricultural film mulching. These results suggest that microbial communities are closely linked to environmental factors such as soil nutrients and PAEs, with PAEs levels significantly influenced by soil environmental conditions.

3.6. Environmentally ecological functions of bacterial communities

All bacterial metabolic and ecologically relevant functions were predicted using the FAPROTAX database. The results showed that 11,922 ASVs were annotated to 59 functional groups across all soil samples, primarily involved in carbon (C), nitrogen (N), and sulfur (S)

cycling (Fig. 9 and Fig. S5). Among these, the functional groups associated with C cycling had the highest abundance, accounting for 40.68 %, followed by N cycling (25.42 %) and S cycling (10.17 %). A total of 24 functional groups were related to C cycling process. Compared to the 0a group, functional groups associated with chemoheterotrophy, aerobic chemoheterotrophy, fermentation, chitinolysis, cellulolysis, methylolysis, and methanol oxidation exhibited higher relative abundances in agricultural film-mulched soil samples. These groups showed a significant increase in the 8a group, followed by a slight decrease, peaking in the 20a group. In contrast, functional groups related to hydrocarbon degradation, photoautotrophy, and anoxygenic photoautotrophy were more abundant in the 0a group. A total of 15 functional groups were annotated as being involved in N cycling process. Nine of these groups reached their maximum abundance in the 3rd year of agricultural film mulching (3a), after which their abundance began to decline. These included nitrate reduction, nitrate respiration, nitrogen respiration, nitrogen fixation, nitrite respiration, nitrate denitrification, nitrite denitrification, nitrous oxide denitrification, and denitrification. The relative abundance of 6 functional groups related to S cycling followed a comparable trend with increasing years of agricultural film mulching. Specifically, the abundance of dark oxidation of sulfur compounds peaked in the 12th year, while the maximum abundance of respiration of sulfur compounds was recorded in the 20th year.

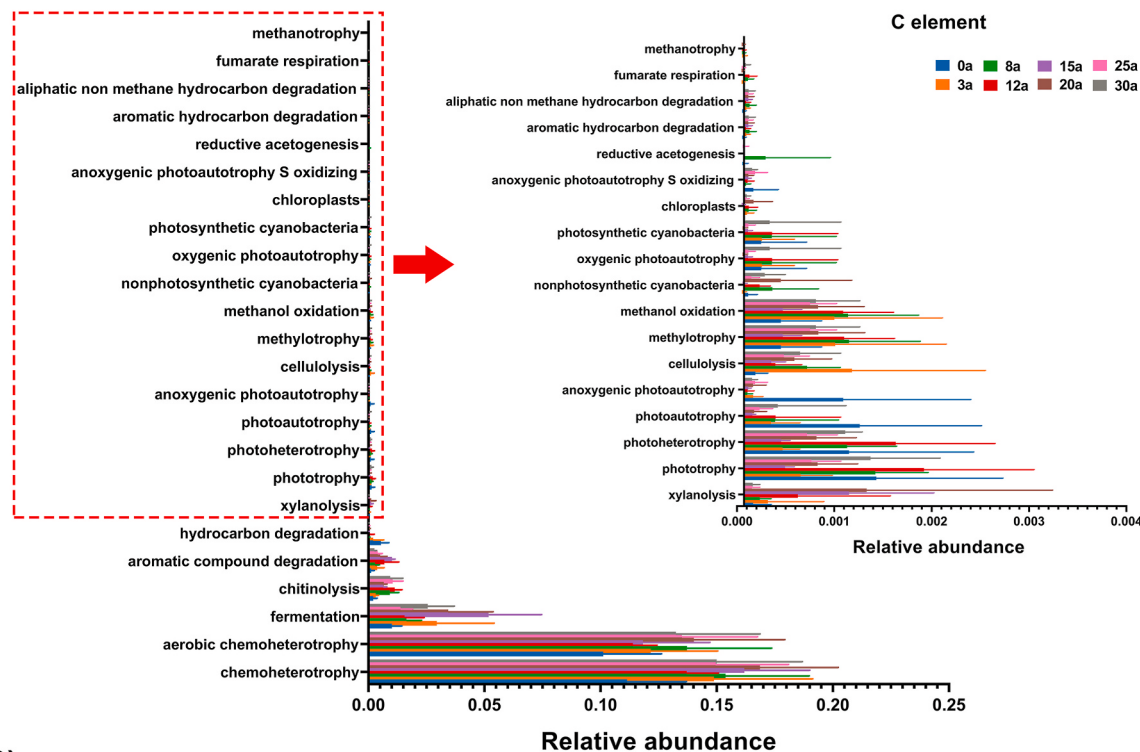
4. Discussion

4.1. Effect of long-term agricultural film mulching on PAEs distribution and soil physicochemical characteristics

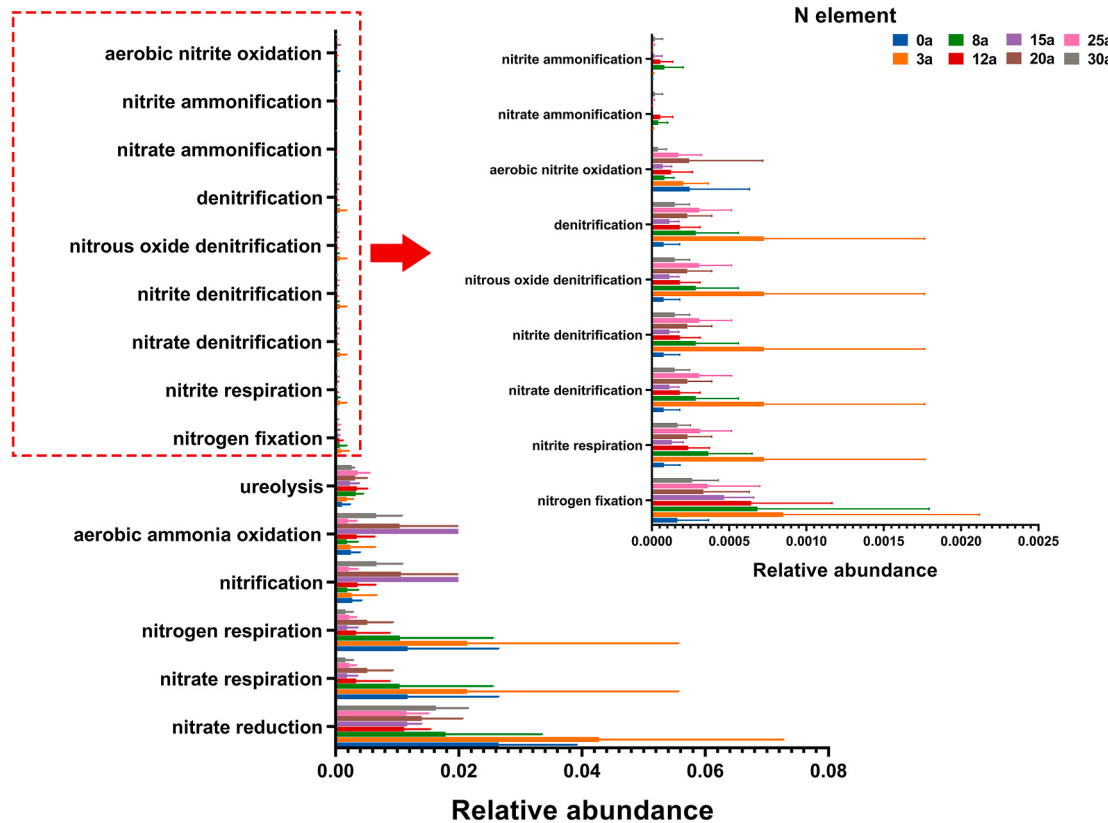
This study reveals the accumulation and migration patterns of PAEs in cotton field soils under varying durations of agricultural film mulching. Over a 30-year period, the concentrations of ΣPAEs demonstrated a transition from an accumulation-dominated (increased PAE concentrations) to a degradation-dominated phase (decreased PAE concentrations), reflecting the complex dynamics of PAEs in the environment. The accumulation of PAEs during the initial mulching period (0–8 years) may be attributed to the ongoing degradation of agricultural film and limited microbial adaptation. After 8 years, the observed degradation of ΣPAEs concentrations may be attributed to the combined effects of several factors. Firstly, the availability of agricultural film material gradually decreases, leading to a reduction in the release of PAEs (Wu et al., 2018). Secondly, the uptake of residual compounds by plants may significantly reduce the concentrations of PAEs in the soil (Zhang et al., 2021a). Enhanced microbial degradation processes are also an important factor. Studies indicate that specific microbial communities exhibit high degradation capacity for PAEs (Chen et al., 2024). In addition, long-term agricultural film mulching may increase soil porosity, facilitating the vertical migration of PAEs into deeper soil layers (Cao et al., 2024). Notably, the persistent accumulation of DEHP and DnOP over a 12-years is closely related to their unique molecular structures and low bioavailability (Arfaeinia et al., 2019). This phenomenon raises concerns about long-chain alkyl PAEs, which are less susceptible to microbial degradation compared to short-chain alkyl PAEs (such as DMP, DEP, and DBP). Due to their more complex structures, long-chain PAEs exhibit greater persistence in the soil (Durante-Rodríguez et al., 2024). Consequently, the removal of these functional groups is a critical step for mitigating the environmental toxicity associated with persistent presence of PAEs. In addition, the strong relationship between DnOP levels and mulching duration emphasizes the long-term ecological consequences of film degradation products on soil health.

Long-term agricultural film mulching significantly altered the physicochemical properties of the soil, resulting in critical changes in soil pH and nutrient dynamics. The observed slight decline in soil pH during the mulching period suggests the potential influence of acidic byproducts generated from the biodegradation of PAEs (Li et al., 2020b).

(A)



(B)

**Fig. 9.** C and N cycling related functions of the bacterial communities as predicted by FAPROTAX.

However, the subsequent recovery of soil pH indicates the soil's inherent buffering capacity, which plays a crucial role in maintaining soil health over time. The impact of PAEs on nutrient cycling is particularly noteworthy, as these compounds appear to modulate microbial communities involved in organic matter utilization and nutrient mineralization processes (Zhu et al., 2018; Li et al., 2023c). This association may contribute to the overall stability and availability of soil nutrients. Additionally, the long-term application of agricultural film mulching correlates with increased concentrations of available nutrients, including AN, AP, and AK. This trend aligns with previous studies indicating that enhanced microbial and root respiration activity fosters the decomposition of organic matter, thus elevating nutrient availability (Shi et al., 2022). While agricultural film mulching appears to benefit soil nutrient levels in cotton fields, the cumulative effects of PAEs on soil ecosystems warrant significant concern. The potential implications for cotton yield and the risks posed to other crop cultivation in the region highlight the necessity for further research into the long-term ecological consequences of such agricultural practices.

4.2. Effect of long-term agricultural film mulching on soil enzyme activity and microbial metabolic activity

The temporal patterns observed in soil enzyme activities reflect the complex impacts of long-term agricultural film mulching on soil biochemical processes. The significant early increases (0–3 years) in enzyme activities, particularly in catalase, alkaline phosphatase, suggest enhanced microbial metabolism and accelerated nutrient cycling. These traits are attributed to a beneficial soil microenvironment enriched with organic matter and available nutrients. The presence of short-chain PAEs likely stimulates microbial activity by providing transient carbon sources, suggesting a complex interplay between anthropogenic inputs and natural soil processes (Chen et al., 2021; Gao et al., 2020). The decline in enzyme activities during prolonged mulching periods (3–8/12 years) aligns with peak PAE concentrations, which are known to exert toxic effects on soil microorganisms. Specifically, compounds such as DEHP and DnOP may inhibit enzyme function by disrupting microbial cell membranes or binding to enzyme active sites, leading to a decrease in enzymatic efficiency (Zhou et al., 2020). Additionally, the reduced availability of labile substrates can diminish microbial demand for enzymes, while soil acidification and structural changes may further limit productive enzyme interactions with substrates. Interestingly, the subsequent recovery in enzyme activity during the later mulching years (12–30 years) suggests an adaptive response by the microbial community, potentially driven by shifts towards taxa capable of degrading PAEs, such as Sphingomonas and Pseudomonas. This recovery phase, along with increases in soil pH and organic carbon content, further promotes the stabilization of the soil environment and a restoration of microbial function and enzyme synthesis. Moreover, the correlations between PAEs and enzyme activities reveal functional linkages that merit further exploration. The positive associations of DnOP and BBP with alkaline phosphatase and catalase indicate their roles in mediating oxidative stress and pollutant degradation, highlighting the ecological ramifications of prolonged PAE exposure.

The findings related to microbial metabolic activity, as evidenced by AWCD analysis, underscore that agricultural film mulching can initially enhance microbial growth and carbon source utilization (3a). However, the mid-term decline (8a and 12a) in microbial activity suggests that lipophilic PAEs from plastic films, a key component of microplastic-related pollutants, significantly alter soil microbial community structures, suppress diversity, and inhibit metabolic pathways by disrupting cell membrane fluidity (Wang et al., 2016). Accordingly, the recovery of microbial activity in the latter years (20a and 25a) of mulching suggests adaptive strategies within soil microbial communities that enable them to metabolize complex carbon compounds from agricultural residues. The ability of soil microorganisms to utilize diverse carbon sources, particularly carbohydrates, amino acids, and carboxylic acids, indicates

a shift towards enhanced metabolic versatility. Carbohydrates, as essential energy sources for microbial growth, along with amino acids and carboxylic acids serving as critical components in biosynthesis and metabolism, play significant roles in maintaining microbial health (Kong et al., 2024). Conversely, the lower utilization rates of phenolic acids and amines imply that these substrates may require specialized enzymatic machinery for effective degradation, suggesting that environmental pollutants and nutrient competition could stifle the production of such enzymes (Temporiti et al., 2022). In conclusion, these findings collectively support the hypothesis that chemicals derived from agricultural plastics act as stressors on soil ecosystems, with profound implications for microbial metabolism and enzyme activity.

4.3. Effect of long-term agricultural film mulching on soil bacterial community

This study highlights the profound impact of long-term agricultural film mulching on the diversity, composition, and structure of soil bacterial community. The early increase (3–8 years) in Shannon and Chao 1 indices reflects that agricultural film residues create new ecological niches, resulting in increased bacterial richness and diversity. This phenomenon indicates that the presence of residues fosters a selective environment in which some bacteria can thrive and potentially improve soil health (Li et al., 2022b). However, the stabilization of bacterial diversity observed in later years, particularly at the 12-year mark, suggests that while initial shifts in community structure occur, these communities eventually reach a dynamic equilibrium. The PCoA and NMDS results reveal that agricultural film residues lead to significant compositional differences when compared to open field soils (0a). The clustering of bacterial communities in soils mulched for 12 years suggests a homogenization effect over time, possibly driven by the selection enrichment of specialized microbial taxa capable of degrading pollutants associated with agricultural film (Sun et al., 2024b; Li et al., 2023a).

The observed shifts in dominant phyla, particularly the increases in Proteobacteria, Actinobacteriota, and Acidobacteriota, further illustrate the adaptive responses of bacterial communities to long-term mulching. These taxa have been identified as key degrading bacteria of farmland mulch in microplastic contaminated soil in Xinjiang, making them relevant in the context of plastic-related bacteria (Ran et al., 2024). Biomarker analysis further revealed the specificity of microbial communities in mulched and open field soils. The presence of these biomarkers suggests their strong adaptability and resistance to the environmental stresses associated with plastic residues. Among them, 8 biomarkers from the phyla Proteobacteria and Acidobacteriota, such as c_Alphaproteobacteria and o_Vicinamibacterales, exhibited notable dominance in mulched soils, possibly due to their roles in plastic degradation and pollutant resistance (Bhattacharyya et al., 2022a). Several Alphaproteobacteria (Sphingomonas yanoikuyae DOS01, Sphingomonas glacialis PAMC 26605, Sphingobium strain SM42) and Vicinamibacterales species were shown to have the ability to metabolize PAEs and degrade complex organic compounds using hydrolytic enzyme (Bhattacharyya et al., 2022a; Ya et al., 2023). In contrast, biomarkers such as BD2_11_terrestrial_group and Balneolales were more abundant in open field soils, reflecting characteristics of relatively undisturbed and natural soil environments without human intervention.

Correlation analysis further revealed the influence of environmental factors in shaping bacterial community composition in agricultural film mulched soils. Alkaline phosphatase, catlase and DnOP were identified as the most influential factors. Among these, alkaline phosphatase was the dominant factor, which aligns with its well-established role in mediating phosphorus cycling and microbial metabolism under environmental stress (Gao et al., 2020). Pearson correlation analysis confirmed that bacterial diversity, as indicated by the Chao 1 and Shannon indices, was significantly influenced by OM, AN, catalase, alkaline phosphatase, DnOP, and the duration of agricultural film mulching. The positive correlations between these factors and bacterial

diversity suggest that they promote microbial richness and evenness, likely by providing diverse ecological niches and substrates (Benjamin et al., 2015). The enrichment of specific biomarkers like Proteobacteria and Acidobacteriota in soils with increasing DEHP and DnOP levels further supports the hypothesis that certain taxa are adapted to PAEs contaminated environments, potentially contributing to their biodegradation.

4.4. Response of bacterial co-occurrence network to long-term agricultural film mulching

To understand the structure of complex bacterial community in long-term agricultural film-mulched soil, co-occurrence network analysis provides valuable insights into the intricate relationships among microbial tax. The observed sustained increase in bacterial network complexity over early mulching periods (0–8/12 years) suggests that soil microbial communities gradually reorganize into more resilient and interconnected network. This adaptability may enhance community stability in response to environmental stresses induced by agricultural practices. However, the decline in network complexity observed in the 15th year suggests that prolonged exposure to environmental stressors can negatively impact bacterial diversity, potentially leading to the loss of sensitive taxa (Liu et al., 2021; Sun et al., 2024a). The subsequent recovery of network complexity by the 25th year illustrates the capacity of soil bacterial communities to adapt and reorganize, accommodating the ongoing presence of plastic degradation byproducts. While co-occurrence networks provide dynamic microbial community interactions, it is essential to recognize that correlation does not imply causation. The identified associations, particularly those involving keystone taxa within the Proteobacteria and Actinobacteriota, serve as valuable starting points for hypothesis generation. Future experimental validation of these interactions, such as through enrichment cultures or stable isotope probing, would provide critical insights into the functional roles of these populations within the community. The ability of certain taxa to form adaptive interactions highlights their potential role as keystone species in stabilizing soil ecosystems under prolonged stress. Further analysis revealed that some bacteria families within the keystone taxa, such as Euzebyaceae, Gemmatimonadaceae, Vicanimacteraceae, and Pyrinomonadaceae, may strengthen the stability of the ecological network and be involved in PAEs degradation pathways (Wang et al., 2023; Zhen et al., 2023). In our future work, we plan to validate key microbial interactions through co-culture assays (e.g., with Sphingomonas, Pseudomonas) and ¹³C-labeled SIP experiments targeting PAEs (e.g., DEHP/DnOP), to track carbon flow into network-identified keystone taxa. These efforts will provide mechanistic confirmation of network-predicted associations and build upon the current study's framework. In summary, while our findings identify potential microbial hubs and ecological roles, experimental approaches are essential to confirm causative interactions.

4.5. Effect of long-term agricultural film mulching on soil ecological functions

The prediction of bacterial metabolic and ecological functions through the FAPROTAX database revealed the significant impact of long-term agricultural film mulching on soil functional bacterial groups involved in C, N, and S cycling. The functional groups associated with C cycling (40.68 %) were predominant, as C cycling is the most important and complex biogeochemical cycle in soil ecosystems (Wang et al., 2022b). The release of PAEs from agricultural films appears to provide alternative carbon sources for microbial communities, influencing processes critical to carbon conversion and organic matter decomposition (Bhattacharyya et al., 2022b). The observed increases in functional groups related to processes such as chemoheterotrophy, aerobic chemoheterotrophy, fermentation, and polysaccharide degradation over time indicate that agricultural film mulching enhances carbon

decomposition mechanisms. This enhancement may be driven by increased organic carbon inputs from root exudates and microbial residues, particularly noted in the 8th and 20th years of mulching (Li et al., 2023b). Functional groups associated with N cycling showed a peak in the 3rd year of mulching, followed by a steady decline. It has been reported that the use of agricultural film can reduce total N abundance in soil, with this effect intensifying as the film ages (Zhang et al., 2021b). Processes such as nitrate reduction, nitrogen fixation, and denitrification were particularly affected. The decline in nitrogen-related functional groups after the initial peak could be attributed to the gradual accumulation of plastic residues, which may disrupt nitrogen mineralization and nitrification processes by inhibiting soil urease (Han et al., 2024). In addition, shifts were also observed in sulfur-related processes such as sulfur oxidation, which increased under long-term mulching, potentially supporting short-term nutrient cycling and plant growth. However, decreases in functional groups associated with hydrocarbon degradation, photoautotrophy, and nitrogen cycling may pose risks to long-term soil ecological stability. It is important to note that the functional predictions presented here are based on 16S rRNA gene sequencing combined with FAPROTAX, which provides putative functional annotations inferred from taxonomic identities. Consequently, these findings should be interpreted as preliminary insights that necessitate further exploration. Future studies employing metagenomic sequencing will be needed for a more accurate and comprehensive characterization of soil microbial functions.

Overall, our findings indicate that continuous mulching leads to the accumulation of PAEs, which can disrupt microbial communities, reduce enzymatic activity, and impair overall soil function. Although signs of recovery in soil health were observed after 12 years of agricultural film application, the persistent presence of PAEs poses ongoing risks to soil ecosystem stability. To address these challenges, it is essential to explore more sustainable agricultural practices. One promising approach is the development and implementation of biodegradable alternatives to traditional polyethylene films. Promoting research and the adoption of these biodegradable mulching materials is crucial for minimizing ecological risks and enhancing the sustainability of agricultural systems. Furthermore, our study highlights the emergence of microbial communities adapted to PAEs, which demonstrate the capacity to tolerate and potentially degrade accumulated pollutants. These adapted microbial taxa represent a valuable biological resource that could be harnessed in future soil bioremediation strategies. Their functional potential may play a crucial role in accelerating the degradation of residual PAEs and restoring soil health in contaminated environments.

5. Conclusion

The results of the present study demonstrated that, with increasing mulching duration, the Σ PAEs content in the soil did not follow a linear growth trend, but instead exhibited a pattern of initial increase followed by a decrease. The peak concentration was observed in the 8th year, reaching 6.40 mg/kg. Furthermore, long-term mulching led to the accumulation of PAEs in the soil, which disrupted the microbial community structure, reduced enzyme activity, and impaired overall soil function. Although signs of soil health recovery were observed after 12 years of mulching, the persistent presence of PAEs suggests that the stability of the soil ecosystem remains at ongoing risk. These findings provide important insights for assessing the dynamic accumulation of PAEs due to long-term mulching and the associated risks of soil pollution. In future studies, we aim to further elucidate the molecular mechanisms underlying PAE-induced changes in soil microbial community structure through multi-omics approaches, such as metagenomics and metabolomics, and to screen for microbial strains with high degradation potential to provide more effective microbial resources for PAE pollution remediation.

CRediT authorship contribution statement

Yuanyang Yi: Writing – review & editing, Writing – original draft, Methodology, Investigation, Funding acquisition, Formal analysis, Conceptualization. **Yuxian Wang:** Writing – review & editing, Visualization, Software, Methodology, Data curation. **Jing Zhu:** Supervision, Formal analysis. **Meiying Gu:** Methodology, Formal analysis, Data curation. **Jianwei Chen:** Visualization, Methodology, Investigation, Data curation. **Ling Jiang:** Validation, Investigation, Data curation. **Delong Kong:** Validation, Investigation. **Zhidong Zhang:** Writing – review & editing, Resources, Formal analysis. **Wei Zhang:** Visualization, Supervision, Project administration, Funding acquisition.

Declaration of competing interest

The authors declare that they have no known competing financial interests or personal relationships that could have appeared to influence the work reported in this paper.

Acknowledgements

This work was supported by the Project of Fund for Stable Support to Agricultural Sci-Tech Renovation (xjnkywdzc-2023005), the National Natural Science Foundation of China (32160002, 2021YFC2102700), the Graduate Student Innovation Fund of Xinjiang Normal University (XJ107622305) and Zhidong Zhang was supported by Tianshan Talent Plan (2022TSYCCX0067).

Appendix A. Supplementary data

Supplementary data to this article can be found online at <https://doi.org/10.1016/j.jenvman.2025.126582>.

Data availability

Data will be made available on request.

References

- Arfaeinia, H., Fazlzadeh, M., Taghizadeh, F., Saeedi, R., Spitz, J., Dobaradaran, S., 2019. Phthalate acid esters (PAEs) accumulation in coastal sediments from regions with different land use configuration along the Persian Gulf. *Ecotoxicol. Environ. Saf.* 169, 496–506. <https://doi.org/10.1016/j.ecoenv.2018.11.033>.
- Alkan, N., Alkan, A., Castro-Jiménez, J., Royer, F., Papillon, L., Ourgaud, M., Sempéré, R., 2021. Environmental occurrence of phthalate and organophosphate esters in sediments across the Gulf of Lion (NW Mediterranean Sea). *Sci. Total Environ.* 760, 143412. <https://doi.org/10.1016/j.scitotenv.2020.143412>.
- Benjamin, S., Pradeep, S., Josh, M.S., Kumar, S., Masai, E., 2015. A monograph on the remediation of hazardous phthalates. *J. Hazard. Mater.* 298, 58–72. <https://doi.org/10.1016/j.jhazmat.2015.05.004>.
- Bhattacharyya, M., Basu, S., Dhar, R., Dutta, T.K., 2022a. Phthalate hydrolase: distribution, diversity and molecular evolution. *Environ. Microbiol. Rep.* 14, 333–346. <https://doi.org/10.1111/1758-2229.13028>.
- Bhattacharyya, S.S., Ros, G.H., Furtak, K., Iqbal, H.M.N., Parra-Saldívar, R., 2022b. Soil carbon sequestration-An interplay between soil microbial community and soil organic matter dynamics. *Sci. Total Environ.* 815, 152928. <https://doi.org/10.1016/j.scitotenv.2022.152928>.
- Cao, J., Gao, X., Zhang, S., Wei, Z., Chen, X., Ma, N., Li, C., Zhao, X., 2024. Migration patterns of phthalic acid esters from mulch plastic film in the soil-plant-atmosphere continuum system. *J. Hazard. Mater.* 480, 136353. <https://doi.org/10.1016/j.jhazmat.2024.136353>.
- Chen, L., Yu, L., Han, B., Li, Y., Zhang, J., Tao, S., Liu, W., 2024. Pollution characteristics and affecting factors of phthalate esters in agricultural soils in mainland China. *J. Hazard. Mater.* 466, 133625. <https://doi.org/10.1016/j.jhazmat.2024.133625>.
- Chen, N., Li, X., Shi, H., Hu, Q., Zhang, Y., Leng, X., 2021. Effect of biodegradable film mulching on crop yield, soil microbial and enzymatic activities, and optimal levels of irrigation and nitrogen fertilizer for the Zea mays crops in arid region. *Sci. Total Environ.* 776, 145970. <https://doi.org/10.1016/j.scitotenv.2021.145970>.
- Dincă, L.C., Grenni, P., Onet, C., Onet, A., 2022. Fertilization and soil microbial community: a review. *Appl. Sci.* 12 (3), 1198. <https://doi.org/10.3390/app12031198>.
- Durante-Rodríguez, G., Francisco-Polanco, S., Fernández-Arévalo, U., Díaz, E., 2024. Engineering bacterial biocatalysts for the degradation of phthalic acid esters. *Microb. Biotechnol.* 17, e70024. <https://doi.org/10.1111/1751-7915.70024>.
- Gao, M., Dong, Y., Zhang, Z., Song, Z., 2020. Effect of dibutyl phthalate on microbial function diversity and enzyme activity in wheat rhizosphere and non-rhizosphere soils. *Environ. Pollut.* 265, 114800. <https://doi.org/10.1016/j.envpol.2020.114800>.
- Han, J., Jiang, Z., Li, P., Wang, J., Zhou, X., 2025. Contamination of phthalic acid esters in China's agricultural soils: sources, risk, and control strategies. *Agronomy* 15 (2), 433. <https://doi.org/10.3390/agronomy15020433>.
- Han, H., Song, P., Jiang, Y., Fan, J., Khan, A., Liu, P., Masek, O., Li, X., 2024. Biochar immobilized hydrolase degrades PET microplastics and alleviates the disturbance of soil microbial function via modulating nitrogen and phosphorus cycles. *J. Hazard. Mater.* 474, 134838. <https://doi.org/10.1016/j.jhazmat.2024.134838>.
- Hu, C., Wang, X., Chen, X., Tang, X., Zhao, Y., Yan, C., 2019. Current situation and control strategies of residual film pollution in Xinjiang. *Trans. Chin. Soc. Agric. Eng.* 35, 223–234. <https://doi.org/10.11975/j.issn.1002-6819.2019.24.027>.
- Hu, R., Zhao, H., Xu, X., Wang, Z., Yu, K., Shu, L., Yan, Q., Wu, B., Mo, C., He, Z., Wang, C., 2021. Bacteria-driven phthalic acid ester biodegradation: current status and emerging opportunities. *Environ. Int.* 154, 106560. <https://doi.org/10.1016/j.envint.2021.106560>.
- Huang, Y.H., Liu, Y., Geng, J., Lü, H., Zhao, H.-M., Xiang, L., Cai, Q.-Y., 2022. Maize root-associated niches determine the response variation in bacterial community assembly and function to phthalate pollution. *J. Hazard. Mater.* 429, 128280. <https://doi.org/10.1016/j.jhazmat.2022.128280>.
- Jiang, J., Gao, X., Lv, Q., Li, Z., Li, P., 2021. Observed impacts of utility-scale photovoltaic plant on local air temperature and energy partitioning in the barren areas. *Renew. Energy* 174, 157–169. <https://doi.org/10.1016/j.renene.2021.03.148>.
- Kapanen, K., Stephen, J.R., Brüggemann, J., Kiviranta, A., White, D.C., Itävärä, M., 2007. Diethyl phthalate in compost: ecotoxicological effects and response of the microbial community. *Chemosphere* 67, 2201–2209. <https://doi.org/10.1016/j.chemosphere.2006.12.023>.
- Kong, M., Huang, M., Zhang, Z., Long, J., Siddique, K.H.M., Zhang, D., 2024. Effects of plastic film mulching on soil microbial carbon metabolic activity and functional diversity at different maize growth stages in cool, semi-arid regions. *Front. Microbiol.* 15, 1492149. <https://doi.org/10.3389/fmicb.2024.1492149>.
- Kong, X., Jin, D., Jin, S., Wang, Z., Yin, H., Xu, M., Deng, Y., 2018. Responses of bacterial community to dibutyl phthalate pollution in a soil-vegetable ecosystem. *J. Hazard. Mater.* 353, 142–150. <https://doi.org/10.1016/j.jhazmat.2018.04.015>.
- Kumari, A., Kaur, R., 2020. A review on morpho-physiological traits of plants under phthalate stress and insights into their uptake and translocation. *Plant Growth Regul.* 91 (3), 327–347. <https://doi.org/10.1007/s10725-020-00625-0>.
- Li, C., Chen, J., Wang, J., Han, P., Luan, Y., Ma, X., Lu, A., 2016. Phthalate esters in soil, plastic film, and vegetable from greenhouse vegetable production bases in Beijing, China: concentrations, sources, and risk assessment. *Sci. Total Environ.* 568, 1037–1043. <https://doi.org/10.1016/j.scitotenv.2016.06.077>.
- Li, X., Liu, W., Zhang, C., Song, P., Wang, J., 2020a. Fate of phthalic acid esters (PAEs) in typical greenhouse soils of different cultivation ages. *Bull. Environ. Contam. Toxicol.* 104 (2), 301–306. <https://doi.org/10.1007/s00128-019-02756-1>.
- Li, W., Wufulier, R., Duo, J., Wang, S., Luo, Y., Zhang, D., Pan, X., 2020b. Microplastics in agricultural soils: extraction and characterization after different periods of polyethylene film mulching in an arid region. *Sci. Total Environ.* 749, 141420. <https://doi.org/10.1016/j.scitotenv.2020.141420>.
- Li, Y., Huang, G., Zhang, L., Gu, H., Lou, C., Zhang, H., Liu, H., 2020c. Phthalate esters (PAEs) in soil and vegetables in solar greenhouses irrigated with reclaimed water. *Environ. Sci. Pollut. Res.* 27, 22658–22669. <https://doi.org/10.1007/s11356-020-08882-2>.
- Li, X., Li, N., Wang, C., Wang, A., Kong, W., Song, P., Wang, J., 2022a. Occurrence of phthalate acid esters (PAEs) in protected agriculture soils and implications for human health exposure. *Bull. Environ. Contam. Toxicol.* 109 (3), 548–555. <https://doi.org/10.1007/s00128-022-03553-z>.
- Li, Y., Yang, R., Guo, L., et al., 2022b. The composition, biotic network, and assembly of plastisphere protistan taxonomic and functional communities in plastic-mulching croplands. *J. Hazard. Mater.* 430, 128390. <https://doi.org/10.1016/j.jhazmat.2022.128390>.
- Li, K., Jia, W., Xu, L., Zhang, M., Huang, Y., 2023a. The plastisphere of biodegradable and conventional microplastics from residues exhibit distinct microbial structure, network and function in plastic-mulching farmland. *J. Hazard. Mater.* 442, 130011. <https://doi.org/10.1016/j.jhazmat.2022.130011>.
- Li, Y., Hou, Y., Hou, Q., Long, M., Yang, Y., Wang, Z., Liao, Y., 2023b. Long-term plastic mulching decreases rhizoplane soil carbon sequestration by decreasing microbial anabolism. *Sci. Total Environ.* 868, 161713. <https://doi.org/10.1016/j.scitotenv.2023.161713>.
- Li, J., Yang, L., Yu, S., Ding, A., Zuo, R., Yang, J., Li, X., Wang, J., 2023c. Environmental stressors altered the groundwater microbiome and nitrogen cycling: a focus on influencing mechanisms and pathways. *Sci. Total Environ.* 895, 167004. <https://doi.org/10.1016/j.scitotenv.2023.167004>.
- Liu, J., Li, S., Yue, S., Tian, J., Chen, H., Jiang, H., Siddique, K.H.M., Zhan, A., Fang, Q., Yu, Q., 2021. Soil microbial community and network changes after long-term use of plastic mulch and nitrogen fertilization on semiarid farmland. *Geoderma* 396, 115086. <https://doi.org/10.1016/j.geoderma.2021.115086>.
- Louca, S., Parfrey, L.W., Doebeli, M., 2016. Decoupling function and taxonomy in the global ocean microbiome. *Science* 353 (6305), 1272–1277. <https://doi.org/10.1126/science.aaf4507>.
- Long, F., Ren, Y., Ji, Y., Li, J., Zhang, H., Wu, Z., Gao, R., Bi, F., Liu, Z., Li, H., 2024. Pollution characteristics, toxicological properties, and health risk assessment of phthalic acid esters in water, soil, and atmosphere. *Atmosphere* 15, 1071. <https://doi.org/10.3390/atmos15091071>.

- Monti, M., Fasano, M., Palandri, L., Righi, E., 2022. A review of European and international phthalates regulation: focus on daily use products. *Eur. J. Publ. Health* 32 (Suppl. 1). <https://doi.org/10.1093/eupub/ckac131.226>.
- Paluselli, A., Kim, S.-K., 2020. Horizontal and vertical distribution of phthalates acid ester (PAEs) in seawater and sediment of East China Sea and Korean South Sea: traces of plastic debris? *Mar. Pollut. Bull.* 151, 110831. <https://doi.org/10.1016/j.marpolbul.2019.110831>.
- Ran, T., Liao, H., Zhao, Y., Li, J., 2024. Soil plastisphere interferes with soil bacterial community and their functions in the rhizosphere of pepper (*Capsicum annuum* L.). *Ecotoxicol. Environ. Saf.* 270, 115946. <https://doi.org/10.1016/j.ecoenv.2024.115946>.
- Shi, M., Kang, Y., Zhang, W., Yang, X., Fan, Y., Yu, H., Zhang, R., Guo, A., Qin, S., 2022. Plastic film mulching with ridge planting alters soil chemical and biological properties to increase potato yields in semiarid northwest China. *Chem. Biol. Technol.* Agric. 9, 16. <https://doi.org/10.1186/s40538-022-00284-5>.
- Sokolowski, A., Kończak, M., Oleszczuk, P., Gao, Y., Czech, B., 2024. Environmental and food contamination by phthalic acid esters (PAEs): overview. *Water Air Soil Pollut.* 235 (5), 313. <https://doi.org/10.1007/s11270-024-07121-5>.
- Sun, Q., Zhang, X., Liu, C., Nier, A., Ying, S., Zhang, J., Shi, M., 2022. The content of PAEs in field soils caused by the residual film has a periodical peak. *Sci. Total Environ.* 864, 161077–161078. <https://doi.org/10.1016/j.scitotenv.2022.161078>.
- Sun, Q., Liu, C., Zhang, X., Wang, Z., Guan, P., Wang, Z., Shi, M., 2024a. Phthalate ester (PAEs) accumulation in wheat tissues and dynamic changes of rhizosphere microorganisms in the field with plastic-film residue. *Sci. Total Environ.* 931, 172833. <https://doi.org/10.1016/j.scitotenv.2024.172833>, 172833.
- Sun, Y., Wu, M., Xie, S., Zang, J., Wang, X., Yang, Y., Wang, J., 2024b. Homogenization of bacterial plastisphere community in soil: a continental-scale microcosm study. *ISME Commun.* <https://doi.org/10.1093/ismeco/ycad012>.
- Tao, R., Zhang, H., Gu, X., Hu, B., Li, J., Chu, G., 2021. Di-(2-ethylhexyl) phthalate (DEHP) exposure suppressed the community diversity and abundance of ammonium oxidizers and mitigated N2O emissions in an alkaline soil. *Ecotoxicol. Environ. Saf.* 227, 112910. <https://doi.org/10.1016/j.ecoenv.2021.112910>.
- Temporiti, M.E., Nicola, L., Girometta, C.E., Roversi, A., Dacco, C., Tosi, S., 2022. The analysis of the mycobiota in plastic polluted soil reveals a reduction in metabolic ability. *J. Fungi* 8, 1247. <https://doi.org/10.3390/jof8121247>.
- Uzamurera, A.G., Wang, P.-Y., Zhao, Z.-Y., Tao, X.-P., Zhou, R., Wang, W.-Y., Xiong, Y.-C., 2023. Thickness-dependent release of microplastics and phthalic acid esters from polyethylene and biodegradable residual films in agricultural soils and its related productivity effects. *J. Hazard Mater.* 448, 130897. <https://doi.org/10.1016/j.jhazmat.2023.130897>.
- Viljoen, S.J., Brailsford, F.L., Murphy, D.V., Hoyle, F.C., Chadwick, D.R., Jones, D.L., 2023. Leaching of phthalate acid esters from plastic mulch films and their degradation in response to UV irradiation and contrasting soil conditions. *J. Hazard. Mater.* 443, 130256. <https://doi.org/10.1016/j.jhazmat.2022.130256>.
- Wang, Z.G., Hu, Y.-L., Xu, W.-H., Liu, S., Hu, Y., Zhang, Y., 2015. Impacts of dimethyl phthalate on the bacterial community and functions in black soils. *Front. Microbiol.* 6, 405. <https://doi.org/10.3389/fmicb.2015.00405>.
- Wang, Y., Liu, L., Zhang, J., Li, D., Yu, J., Gao, H., Li, H., Zhao, Z., 2022a. Soil phytoremediation reveals alteration in soil microbial metabolic activities along time gradient of cover crop mulching. *Environ. Res.* 209, 112884. <https://doi.org/10.1016/j.envres.2022.112884>.
- Wang, J., Lv, S., Zhang, M., Chen, G., Zhu, T., Zhang, S., Teng, Y., Christe, P., Luo, Y., 2016. Effects of plastic film residues on occurrence of phthalates and microbial activity in soils. *Chemosphere* 151, 171–177. <https://doi.org/10.1016/j.chemosphere.2016.02.076>.
- Wang, C., Yao, X., Li, X., Wang, Q., Wang, J., Zhu, L., Wang, J., 2023. Effects of dibutyl phthalate on microbial community and the carbon cycle in salinized soil. *J. Clean. Prod.* 404, 136928. <https://doi.org/10.1016/j.jclepro.2023.136928>.
- Wang, S., Jin, Z., Li, X., Zhu, H., Fang, F., Luo, T., Li, J., 2025. Characterization of microbial carbon metabolism in karst soils from citrus orchards and analysis of its environmental drivers. *Microorganisms* 13 (2), 267. <https://doi.org/10.3390/microorganisms13020267>.
- Wang, Y., Zhang, Q., Han, Y., Zhang, D., Zhang, C., Hu, C., 2022b. Carbon cycle in the microbial ecosystems of biological soil crusts. *Soil Biol. Biochem.* 171, 108729. <https://doi.org/10.1016/j.soilbio.2022.108729>.
- Wu, Y., Chen, X., Zhu, T., Li, X., Chen, X., Mo, C., Li, Y., Cai, Q., Wong, M., 2018. Variation in accumulation, transport, and distribution of phthalic acid esters (PAEs) in soil columns grown with low- and high-PAE accumulating rice cultivars. *Environ. Sci. Pollut. Res.* 25, 17768–17780. <https://doi.org/10.1007/s11356-018-1938-x>.
- Ya, H., Zhang, T., Xing, Y., Lv, M., Wang, X., Jiang, B., 2023. Co-existence of polyethylene microplastics and tetracycline on soil microbial community and ARGs. *Chemosphere* 335, 139082. <https://doi.org/10.1016/j.chemosphere.2023.139082>.
- Yang, H., Hu, Z., Wu, F., Guo, K., Gu, F., Cao, M., 2023. The use and recycling of agricultural plastic mulch in China: a review. *Sustainability* 15 (20), 15096. <https://doi.org/10.3390/2021-1050/15/20/15096>.
- Yang, Q., Wu, Y., Zhang, S., Xie, H., Han, D., Yan, H., 2025. Recent advancements in the extraction and analysis of phthalate acid esters in food samples. *Food Chem.* 463, 141262. <https://doi.org/10.1016/j.foodchem.2024.141262>.
- Zhang, Q., Ma, Z., Cai, Y., Li, H., Ying, G., 2021a. Agricultural plastic pollution in China: generation of plastic debris and emission of phthalic acid esters from agricultural film. *Environ. Sci. Technol.* 55, 12459–12470. <https://doi.org/10.1021/acs.est.1c04369>.
- Zhang, X., Li, Y., Ouyang, D., Lei, J., Tan, Q., Xie, L., Li, Z., Liu, T., Xiao, Y., Farooq, T.H., Wu, X., Chen, L., Yan, W., 2021b. Systematical review of interactions between microplastics and microorganisms in the soil environment. *J. Hazard. Mater.* 418, 126288. <https://doi.org/10.1016/j.jhazmat.2021.126288>.
- Zhang, W., Xu, J., Zhu, L., Wu, L., Luo, Y., 2023. Effects of fertilizer application on phthalate ester pollution and the soil microbial community in plastic-shed soil on long-term fertilizer experiment. *J. Hazard. Mater.* 452, 131251. <https://doi.org/10.1016/j.jhazmat.2023.131251>.
- Zhen, Z., Luo, S., Chen, Y., Li, G., Li, H., Wei, T., Huang, F., Ren, L., Liang, Y., Lin, Z., Zhang, D., 2023. Performance and mechanisms of biochar-assisted vermicomposting in accelerating di-(2-ethylhexyl) phthalate biodegradation in farmland soil. *J. Hazard. Mater.* 443, 130330. <https://doi.org/10.1016/j.jhazmat.2022.130330>.
- Zhou, B., Zhao, L., Wang, Y., Sun, Y., Li, X., Xu, H., Weng, L., Pan, Z., Yang, S., Chang, X., Li, Y., 2020. Spatial distribution of phthalate esters and the associated response of enzyme activities and microbial community composition in typical plastic-shed vegetable soils in China. *Ecotoxicol. Environ. Saf.* 195, 110495. <https://doi.org/10.1016/j.ecoenv.2020.110495>.
- Zhu, F., Zhu, C., Doyle, E., Liu, H., Zhou, D., Gao, J., 2018. Fate of di-(2-ethylhexyl) phthalate in different soils and associated bacterial community changes. *Sci. Total Environ.* 637–638, 460–469. <https://doi.org/10.1016/j.scitotenv.2018.05.055>.